

The biotic crisis across the Oceanic Anoxic Event 2: Palaeoenvironmental inferences based on foraminifera and geochemical proxies from the South Iberian Palaeomargin



Matias Reolid ^{a,*}, Carlos A. Sánchez-Quiñónez ^b, Laia Alegret ^c, Eustoquio Molina ^c

^a Departamento de Geología and CEACT, Universidad de Jaén, Campus Las Lagunillas sn, 23071 Jaén, Spain

^b Departamento de Geociencias, Universidad Nacional de Colombia, Bogotá, Carrera 30, n° 45-03, Colombia

^c Departamento de Ciencias de la Tierra e IUCA, Universidad de Zaragoza, Pedro Cerbuna 12, 50009 Zaragoza, Spain

ARTICLE INFO

Article history:

Received 24 March 2015

Received in revised form

28 September 2015

Accepted in revised form 11 October 2015

Available online 17 December 2015

Keywords:

Trophic conditions

Redox conditions

Foraminifera

OAE2

Cretaceous

ABSTRACT

Open marine sediments deposited during the Cenomanian–Turonian transition are well exposed in the Spanish Baños de la Hedionda section (Betic Cordillera, South Iberian Palaeomargin). Analysis of foraminiferal assemblages and geochemical proxies allow inferences on the impact of the Oceanic Anoxic Event 2 (OAE2) in this area of the western Tethys. Three main intervals have been identified corresponding to different lithological units and biozones. (1) The top of the Capas Blancas Member (*Rotalipora cushmani* Biozone) represents the pre-extinction phase with diverse foraminiferal assemblages and well developed water-column tiering, well-oxygenated, oligotrophic deep-waters and oxygenated to poorly oxygenated, mesotrophic surface-waters. Foraminiferal opportunist species point to a minor event with dysoxic conditions preceding the OAE2. (2) The black radiolaritic shales (*Whiteinella archaeocretacea* Biozone) consist of a foraminiferal-barren interval, except for the lowermost centimetres where planktic surface-dweller opportunists are common. Redox sensitive elements (Cr/Al, V/Al, U/Th, Mo_{EF}, Mo_{aut}, U_{EF} and U_{aut}) and increased TOC values reflect oxygen depleted conditions related to the OAE2. The increase in P/Ti values at the base of this stratigraphic interval indicates an abrupt increase in productivity. High concentrations of radiolarians are congruent with high surface productivity probably related to changes in oceanic circulation and enhanced upwelling currents, as well as subsequent shallowing of the oxygen-minimum zone. The increase in Mo_{EF} and Mo_{aut} towards the top of the black radiolaritic shales indicates temporal euxinic conditions. (3) A slow, bottom-up recovery of foraminiferal assemblages is inferred at the base of the Boquerón Member (*Helvetoglobotruncana helvetica* Biozone), with seafloor recolonization by benthic foraminifera being recorded previous to the water column colonization by planktic forms, mainly by intermediate-dwellers typical of mesotrophic waters. The subsequent proliferation of surface-dweller opportunists and deep-dweller opportunists adapted to mesotrophic to eutrophic conditions, and the decrease in planktic foraminiferal diversity, may indicate the persistence of poorly oxygenated conditions in the water column towards the lower-middle part of the *H. helvetica* Biozone.

© 2015 Elsevier Ltd. All rights reserved.

1. Introduction

Oceanic Anoxic Event 2 (OAE2) is represented by the worldwide deposition of organic-rich facies across the Cenomanian/Turonian (C/T) boundary and has been related to palaeoceanographic and climatic changes including greenhouse warming (e.g. Huber et al., 1999, 2002; Norris et al., 2002; Bornemann et al., 2008; Tsandev

and Slomp, 2009; Monteiro et al., 2012; Pogge von Strandmann et al., 2013), a perturbation of the global carbon cycle (e.g. Kuypers et al., 2002; Erba, 2004; Pogge von Strandmann et al., 2013), a sea-level transgression (Hallam, 1992), and a probable massive magmatic episode (e.g. Kuroda et al., 2007; Turgeon and Creaser, 2008; Erba et al., 2013). In the marine realm, both planktic and benthic foraminifera were affected by OAE2. The planktic foraminiferal turnover (Coccioni and Luciani, 2004; Caron et al., 2006) includes the disappearance of the genus *Rotalipora* close to the OAE2 (e.g. Hart, 1996, 1999; Nederbragt and Fiorentino, 1999; Keller et al., 2001; Coccioni and Luciani, 2004; Reolid et al.,

* Corresponding author.

E-mail address: mreolid@ujaen.es (M. Reolid).

2015). Planktic foraminifera are sensitive to temperature, chemical and trophic conditions of the seawater column, and the ecostratigraphic analysis of their assemblages may be used to reconstruct palaeoceanographic changes across the OAE2 (e.g. Jarvis et al., 1988; Huber et al., 1999; Coccioni and Luciani, 2004; Gebhardt et al., 2004, 2010). In addition, the ecostratigraphic analysis of benthic foraminiferal assemblages is a useful tool to interpret paleoenvironmental fluctuations at the seafloor (e.g. Bernhard, 1986; Koutsoukos et al., 1990; Nagy, 1992; Jorissen et al., 1995; Van der Zwaan et al., 1999; Klein and Mutterlose, 2001; Reolid et al., 2008a, 2012a,b). Some authors have interpreted an extinction event affecting benthic foraminiferal assemblages at the C/T boundary (e.g. Kaiho, 1994, 1999; Peryt and Lamolda, 1996; Peryt, 2004), but there is disagreement whether this occurred globally (Holbourn and Kuhnt, 2002).

The analysis of redox-sensitive trace elements such as Cr, Mo and V, among others, has proved to be a useful tool for interpreting redox conditions during oceanic anoxic events. These elements are less soluble under reducing conditions, resulting in syndimentary enrichments under oxygen-depleted conditions (Wignall and Myers, 1988; Calvert and Pedersen, 1993; Jones and Manning, 1994; Powell et al., 2003; Gallego-Torres et al., 2007; Reolid et al., 2012a,b, 2015). Geochemical proxies have also been successfully applied to interpret palaeoproductivity, the most extensively used being the Ba/Al and P/Ti ratios (e.g., Turgeon and Brumsack, 2006; Gallego-Torres et al., 2007; Robertson and Filippelli, 2008; Sun et al., 2008; Reolid and Martínez-Ruiz, 2012; Reolid et al., 2012a,b). The total organic carbon (TOC) has also been employed as an indirect palaeoproductivity proxy (e.g., Gupta and Kawahata, 2006; Su et al., 2008), although enhanced TOC content may result from oxygen depletion and poor bottom-water ventilation.

The aim of this work is to integrate foraminiferal data and geochemical proxies to interpret the palaeoenvironmental turnover across the OAE2 in the Baños de la Hedionda section (Betic Cordillera, southern Spain). The OAE2 and the Cenomanian–Turonian (C–T) transition are recorded in the Betic Cordillera, where studies on foraminifera, calcareous nannoplankton, radiolarian and trace fossils have been carried out (e.g. Rodríguez-Tovar et al., 2009a,b; Sánchez-Quiñónez et al., 2010). Here we present the first integrated analysis of benthic and planktic foraminiferal assemblages and geochemical proxies across the C–T transition from the Baños de la Hedionda section.

2. Geological setting

The studied section (36°23'39"N, 5°15'45"W) is located in the Málaga province (southern Spain), 1 km north from Manilva village (Fig. 1). The studied section belongs to the Penibetic, i.e., the External Zones of the Betic Cordillera (Fig. 1). The Betic Cordillera is the westernmost Alpine Mediterranean Chain together with the Rifian Cordillera in north Morocco. The Betic Cordillera is divided into internal and external zones, the last one formed by thin-skinned thrust sheets detached from their basement and consisting of thick successions of Triassic to Miocene sedimentary rocks (Vera, 2004). The Betic External Zones comprise the Prebetic and Subbetic, which constituted epicontinental and epiocceanic environments, respectively, beginning in the Early Jurassic. The Baños de la Hedionda section is located in the westernmost part of the Internal Subbetic, also called the Penibetic, which constituted a moderately deep pelagic plateau located in the most distal part of the South Iberian palaeomargin (Martín-Algarra, 1987).

The Baños de la Hedionda section is located in the eastern limb of the N–S trending Canutos de la Utrera anticline, which constitutes a tectonic window among the Cretaceous–Tertiary turbiditic successions of the Campo de Gibraltar Flysch Complex. The

succession is composed of thick limestones of the Líbar Group, surrounded by marly limestones and marls of the Espartina Group. The top of the Líbar Group is capped by a decimetre-thick pelagic limestone bed with phosphate deposits (stromatolites and macro-oncoids) of the latest Valanginian–earliest Hauterivian (González-Donoso et al., 1983; Martín-Algarra and Vera, 1994; Martín-Algarra and Sánchez-Navas, 2000). The Espartina Group includes the Capas Blancas and the Capas Rojas formations, represented by scaglia-type facies consisting of white and red pelagic marly limestones and marls rich in chert nodules and layers, and characterized by the abundance of planktic foraminifera. The Capas Blancas Formation (~54 m thick) is subdivided in the Capas Blancas Member (~36 m thick) and Boquerón Member (~16 m thick), which are separated by a <1.5 m thick bituminous interval that consists of black shales and black radiolaritic interlayers (Martín-Algarra, 1987).

The studied interval (Fig. 1C) is 6 m thick and belongs to the upper part of the Capas Blancas Formation. The lowermost 3.2 m consist of marls and marly-limestones with local chert nodules of the Capas Blancas Member (Figs. 1C and 2). These sediments are overlain by 1.45 m of black radiolaritic shales composed by thin laminated black clays and black radiolaritic cherts (Figs. 1C and 2). The uppermost 1.3 m of the studied section consist of white limestones with chert nodules and marls, and belong to the Boquerón Member (Fig. 1C and 2).

3. Material and methods

Lithofacies and microfacies were analysed by field observations and from a total of 19 thin sections and 2 polished slabs. Foraminiferal and geochemical analyses were conducted in a total of 28 sampling levels across the 6 m thick, C–T transition (Fig. 1).

Micropalaeontological samples were disaggregated in water with diluted H₂O₂, washed through a 63 µm sieve, and dried at 50 °C. More indurated limestones were immersed in acetic acid (80%) during 1–4 h, depending on the carbonate content, then washed through a 63 µm sieve, and dried at 50 °C. Quantitative studies were based on representative splits (using a modified Otto microsplitter) of over 300 specimens of benthic foraminifera and 300 specimens of planktic foraminifera larger than 63 µm per sample. The remaining residue was scanned for rare species. Simple diversity (number of species) and the Fisher- α diversity index (e.g. Murray, 1991) were calculated separately for benthic and planktic foraminiferal assemblages. Most of the planktic specimens in relatively more indurated limestones and marly-limestones samples are poorly preserved, mainly due the acetic acid immersion. For this reason, quantification of planktic foraminifera was carried out only at the genus level. The studied specimens are curated in the institutional repository of the Laboratorio de Micropaleontología of the Universidad Nacional de Colombia (Bogotá, Colombia) and constitute the “Baños de la Hedionda Planktics” Collection with the identification BH-2014-00pl to BH-2014-89pl and “Baños de la Hedionda Benthics” Collection with the identification BH-2014-00bent to BH-2014-89bent. Specimens were photographed and illustrated using a Scanning Electron Microscope Zeiss PE Merlin at the University of Zaragoza. Some images were taken with an optical microscope with a digital charge-coupled device (ccd) camera, the resulting image being a composite picture from digital images taken at several focus depth slices (~30 images for larger specimens, see Hanagata and Nobuhara, 2015).

We used the morphogroup analysis of benthic foraminifera (e.g., Corliss, 1985; Jones and Charnock, 1985; Corliss and Chen, 1988) combined with the comparison of fossil and recent communities as an approach to infer probable microhabitat preferences and environmental parameters (e.g., Bernhard, 1986; Fontanier et al., 2002;

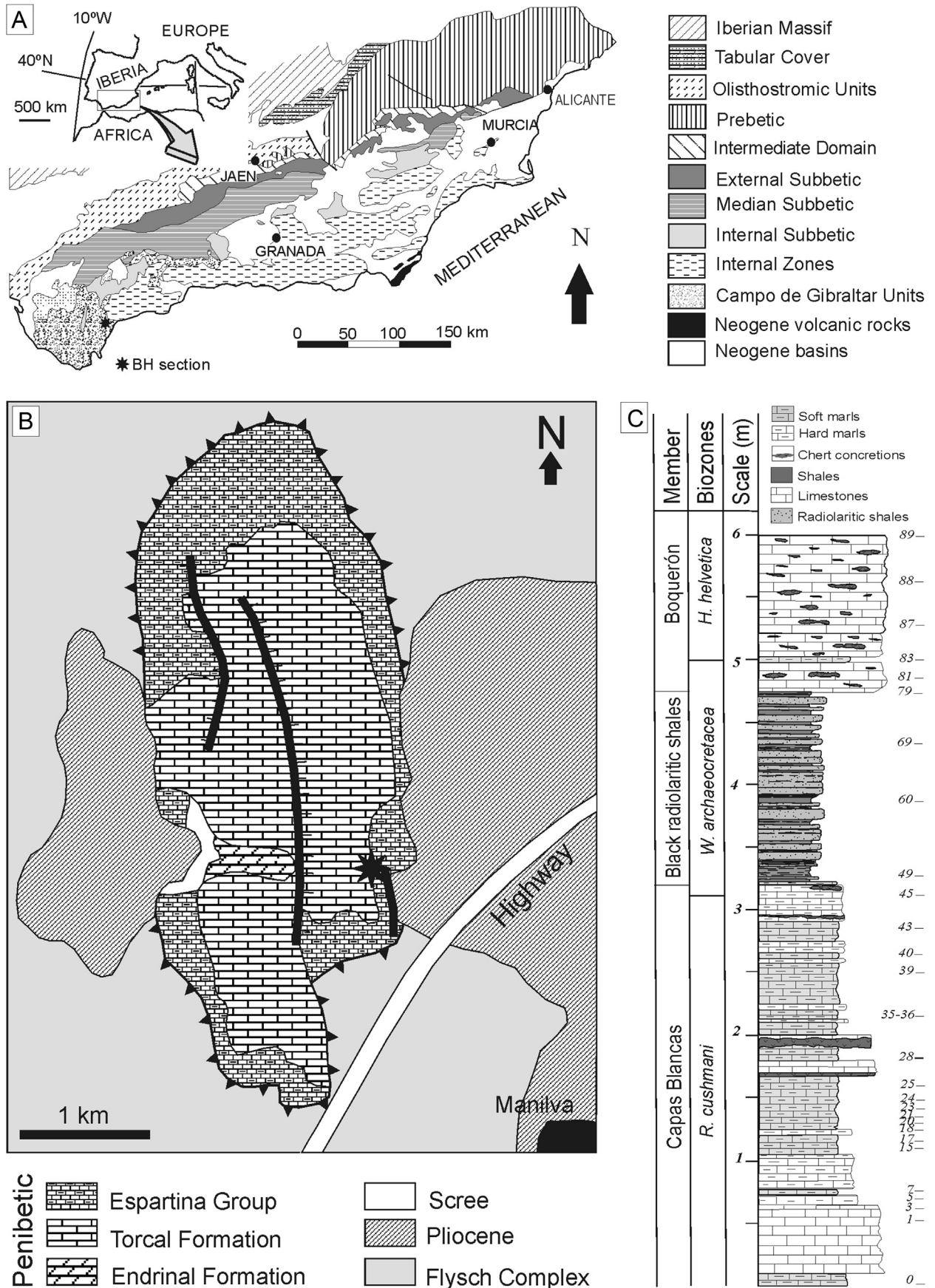


Fig. 1. (A) Geological setting of the Betic Cordillera, (B) detailed geological setting of the studied section (star) close to Manilva village, (C) Baños de la Hedionda section including the lithostratigraphic units, foraminiferal biozones and location of the samples.

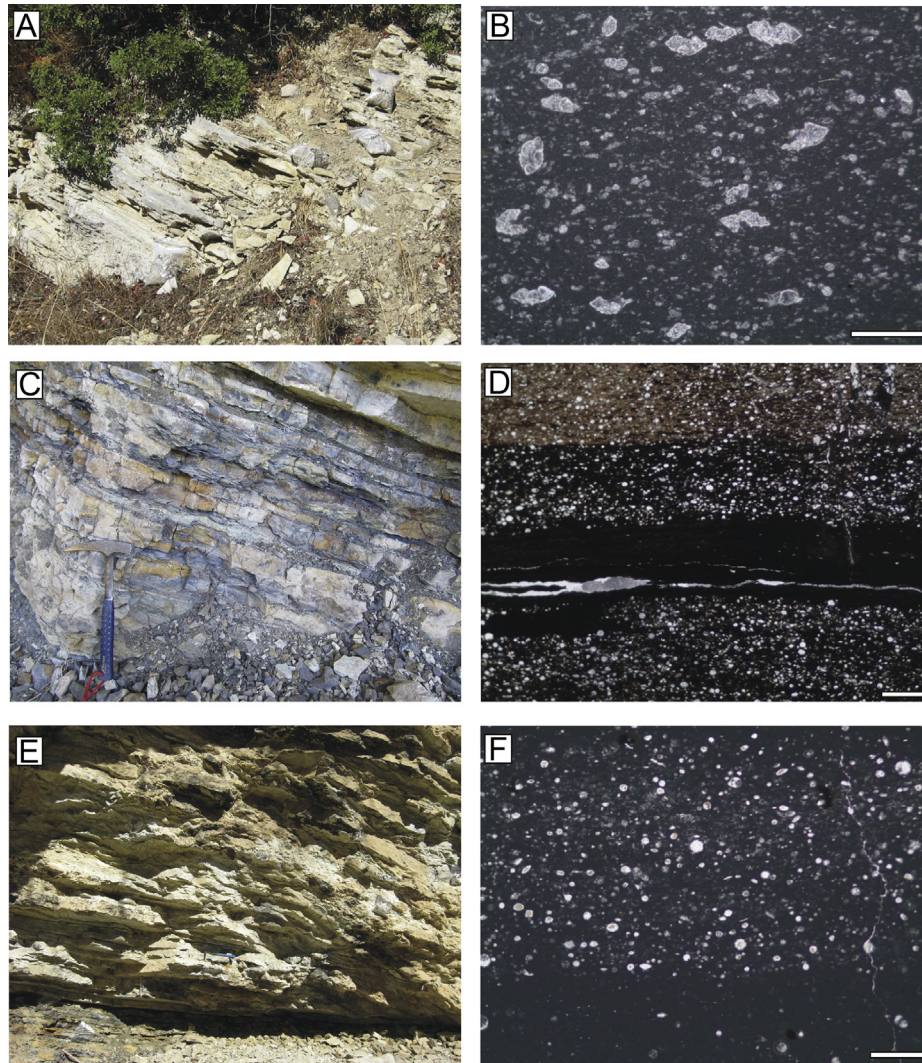


Fig. 2. Macroscopic view of the lithostratigraphic units and microfacies. Capas Blancas Member (A) and (B), black radiolaritic shales (C) and (D), and Boquerón Member (E) and (F). Scale bar 1 mm.

Jorissen et al., 2007). Uncertainties regarding the microhabitat for many recent deep-sea species (e.g., Buzas et al., 1993), however, and the fact that we do not know to what extent the Cretaceous faunas were analogous to recent faunas, suggest that caution must be taken with the interpretation of these comparisons (e.g., Jorissen et al., 2007), and only major changes in morphogroups have been considered to be significant (Gooday, 2003). Planktic foraminiferal morphogroups and inferred life style including redox and trophic requirements are based on Hart and Bailey (1979), Hart (1999), Keller et al. (2001) and Coccioni and Luciani (2004). The life styles of helvetoglobotruncanids, praeglobotruncanids, dicarinelids and hedbergellids have been updated according to Ando et al. (2010), Wendler et al. (2013) and Huber and Petrizzo (2014).

Whole-rock analyses of major elements were carried out in 28 samples using X-ray fluorescence (XRF) in a Philips PW 1040/10 spectrometer. The content of trace elements was determined using an inductively coupled plasma-mass spectrometer (ICP-MS Perkin Elmer Sciex-Elan 5000) at the Centro de Instrumentación Científica (CIC, Universidad de Granada). Instrumental error was $\pm 2\%$ and $\pm 5\%$ for respective elemental concentrations of 50 ppm and 5 ppm.

The contents in C, N and S, as well as the total organic carbon (TOC) content, were analysed with an Elemental Analyzer LECO

CNS-TruSpec and an Inorganic Carbon Analyzer CM5240 UIC in the laboratories of the Centro Andaluz de Medio Ambiente (CEAMA, Granada). Total organic carbon was obtained as the difference between total carbon and total inorganic carbon; it was measured in mg and calculated as percentage of sample weight.

In order to compare trace-element proportions in samples with varying carbonate and clay contents, trace-element concentrations were normalized to aluminium content (Calvert and Pedersen, 1993). This technique avoids any lithological effects on trace or major element concentrations, assuming that Al content in sediments is heightened by aluminosilicates (e.g., Calvert, 1990). The study of palaeoproductivity was carried out applying two palaeoproductivity proxies, Ba/Al and P/Ti. To analyse palaeo-oxygenation, two redox proxies evaluating the relative increase of redox sensitive elements, Cr/Al and V/Al, were applied throughout the section as well as the enrichment factors of Mo and U. According to Zhou et al. (2012) and Tribouillard et al. (2012), the enrichment factors are calculated as $Mo_{EF} = [Mo/Al]_{sample}/[Mo/Al]_{PAAS}$ and $U_{EF} = [U/Al]_{sample}/[U/Al]_{PAAS}$. The authigenic values of U and Mo were also calculated according to Zhou et al. (2012), as $Mo_{aut} = [Mo]_{sample} - [Mo]_{PAAS}/[Al]_{PAAS} * [Al]_{sample}$, $U_{aut} = [U]_{sample} - [U]_{PAAS}/[Al]_{PAAS} * [Al]_{sample}$.

4. Results

4.1. Microfacies

The top of the Capas Blancas Member corresponds to light (locally dark grey) marls and light grey marly limestones in decimetre-thick beds with black chert nodules and interlayers (Fig. 2A). The microfacies range from mudstones to laminated packstones rich in planktic foraminifera and radiolarids (Fig. 2B).

The black radiolaritic shale interval is characterized by very dark coloured clay-rich layers and radiolaritic layers (Fig. 2C). Thin lamination is persistent in both clay-rich layers and radiolarites. The lower part (from 0 to 45 cm) is composed of black clayey radiolarites and dark grey or black silicified shales (both in beds <5 cm thick). The middle interval (from 45 to 100 cm) contains 10 cm of black shales at the bottom, and is characterized by the dominance of black and grey radiolarites with well-laminated black shales interlayers. The upper interval (100–145 cm) contains alternations of black and grey radiolarites with black and dark grey shales (Figs. 2C and D). The top of the black radiolaritic shale interval consists of a 4 cm thick horizon of green clays, overlain by the cherty limestone beds of the Boquerón Member.

The base of the Boquerón Member is more calcareous and rich in chert nodules than the top of the Capas Blancas Member, but radiolarians are very common (Figs. 2E and F).

4.2. Planktic foraminifera and biostratigraphy

For biostratigraphic assignments, we follow the planktic foraminiferal biozones proposed by Robaszynski and Caron (1995) for the Cretaceous in Europe and the Mediterranean. According to the definition of the GSSP (Global Stratotype Section and Point) for the base of the Turonian stage (Kennedy et al., 2005), the C/T boundary is located within the *Whiteinella archaeocretacea* Biozone.

The *Rotalipora cushmani*, *Whiteinella archaeocretacea* and *Helvetoglobotruncana helvetica* biozones have been recognized at the Baños de la Hedionda section. The *R. cushmani* Biozone (upper Cenomanian) corresponds to the studied interval of the Capas Blancas Member, except for its uppermost centimetres. This biozone is characterized by trochospiral keeled planktic forms such as *Rotalipora cushmani*, *Rotalipora montsalvensis*, *Thalmaninella greenhornensis*, *Thalmaninella brotzeni*, *Parathalmaninella appenninica*, and *Thalmaninella deecke*. The *W. archaeocretacea* Biozone includes the topmost centimetres of the Capas Blancas Member, the black radiolaritic shales and the lowermost centimetres of the Boquerón Member. The most common species of this biozone are *Praeglobotruncana stephani*, *Praeglobotruncana gibba*, *Muricohedbergella delrioensis*, and *Marginotruncana sigali*. According to O'Dogherty (1994) and O'Dogherty et al. (2001) a sudden renewal of radiolarian species in this section delineates the boundary between *Guttacapsa biacuta* Biozone and *Alievium superbum* Biozone, which correlates approximately to the *Whiteinella archaeocretacea* Biozone. The lower Turonian *H. helvetica* Biozone includes the uppermost metre of the Boquerón Member. This biozone is characterized by the record of *Helvetoglobotruncana helvetica*, *Helvetoglobotruncana prae-helvetica* and *Guembelitra cenomana*. Other characteristic species recorded within this biozone include *Marginotruncana marginata*, *Sigalitruncana marianosi* and *Whiteinella inornata*.

Planktic foraminiferal assemblages (Fig. 3) are abundant and diverse across the studied section except for the black radiolaritic shales unit, which is barren of foraminifera (Figs. 4 and 5; Table 1). A total of 14 genera and 34 species have been recorded.

The Capas Blancas Member (samples BH-0 to BH-45) shows P/B (planktic/benthic foraminifera) values ranging from 97 to 99%

(Fig. 4). The number of species of planktic foraminifera is high (17–22 species/sample) and the Fisher- α index of diversity ranges between 3.76 and 5.37 (Fig. 4). According to planktic morphogroups (Fig. 6), assemblages are dominated by trochospiral morphogroups in the Capas Blancas Member (83.4–94.2%), while planispiral morphogroups make up between 4.7 and 13.1% of the assemblages (Fig. 7). Keeled trochospiral forms dominate over unkeeled forms. Biserial forms are a minor component of the assemblages (less than 5%). The most common species include *Praeglobotruncana stephani*, *Thalmaninella brotzeni*, *Praeglobotruncana gibba*, *Rotalipora cushmani*, *Muricohedbergella delrioensis*, *Muricohedbergella planispira*, *Muricohedbergella simplex*, and *Globigerinelloides bentonensis*. The relative abundance of the *Dicarinella*, *Muricohedbergella* and *Whiteinella* decrease towards the upper half of the Capas Blancas Member, while the proportions of *Praeglobotruncana* (mainly *P. gibba* and *P. stephani*) and *Rotalipora* (mainly *R. cushmani*) increase (Fig. 8). Two species disappear in the lower half of this member: *Dicarinella algeriana* reappears higher up in the section, and *Whiteinella aumalensis* has not been observed in any other samples across the studied section.

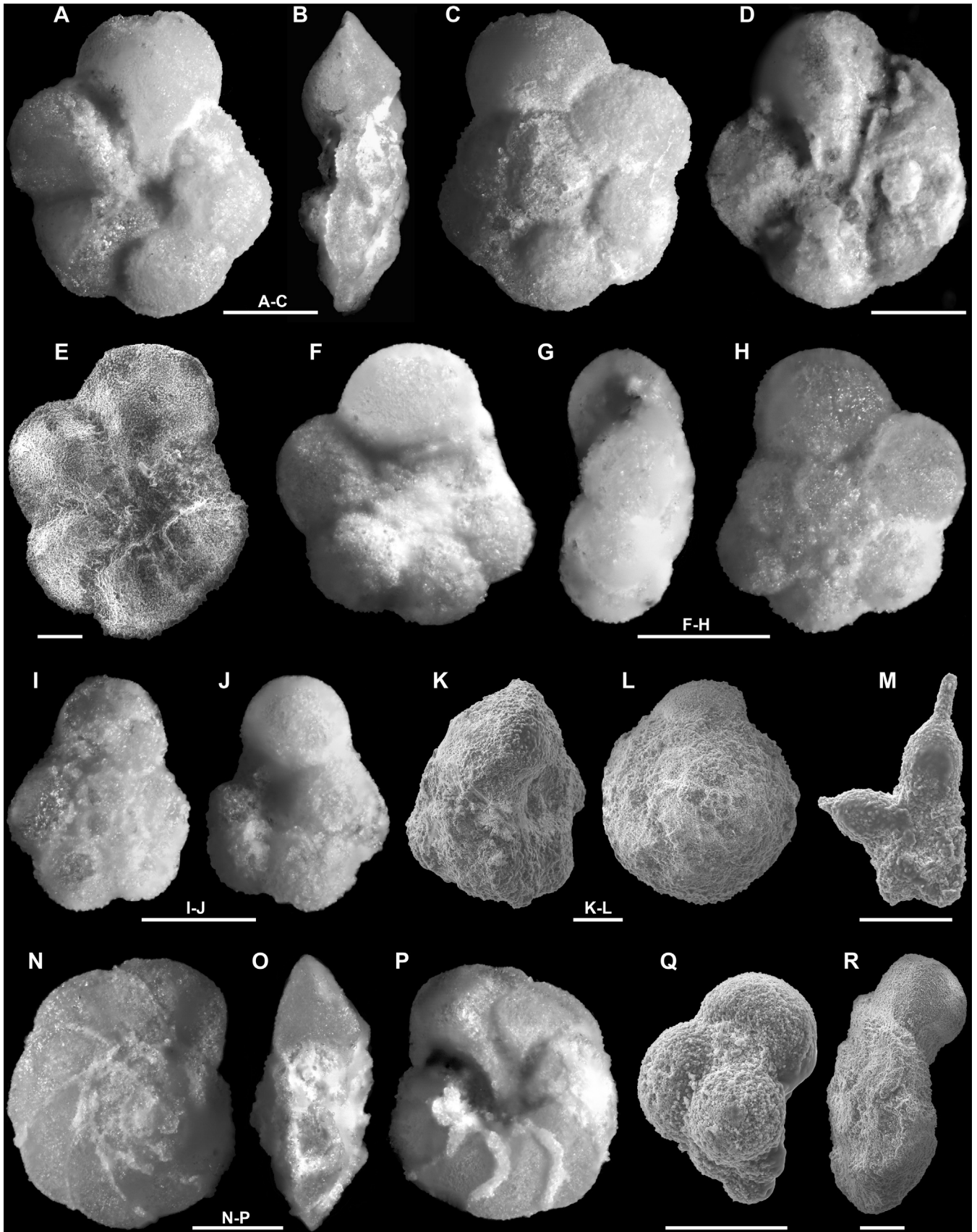
The black radiolaritic shales constitute a barren interval except for the lowermost sample (BH-49), which contains very scarce planktic foraminifera that belong to 4 species (*Muricohedbergella delrioensis*, *Marginotruncana sigali*, *Praeglobotruncana stephani* and *P. gibba*) but no benthic taxa. The low-diversity (Fisher- α = 2.62, Fig. 4) foraminiferal assemblage is dominated by trochospiral morphogroups (86.7%), mainly keeled forms, followed by planispiral morphogroups (13.3%, Fig. 7). Biserial and triserial planktic foraminifera are not recorded. *Muricohedbergella delrioensis* becomes more abundant in this sample with respect to the underlying Capas Blancas Member, and the species *Marginotruncana sigali* first occurs.

The lowermost 50 cm of the Boquerón Member are also barren of planktic foraminifera (Figs. 4, 5, 7 and 8). The P/B ratio across the rest of this unit is high, but it drops down to 0% in sample BH-88 (Fig. 4). The number of planktic species ranges from 11 to 22 species/sample, and the Fisher- α index ranges between 2.99 and 5.48 (Fig. 4). Unkeeled trochospiral forms replace keel trochospiral ones in the upper half of this member (Fig. 7). Biserial and triserial morphogroups are a minor component of the assemblages, and planispiral forms are recorded only in the lowermost sample (BH-83). *Whiteinella baltica*, *Praeglobotruncana stephani*, *Praeglobotruncana gibba*, *Muricohedbergella delrioensis* and *Dicarinella algeriana* are the most common species (Fig. 8). The lower half of the Boquerón Member is characterized by high percentages of *Dicarinella*, which is scarcely recorded in the Capas Blancas Member. The genera *Planoheterohelix* and *Guembelitra* first occur at the base of the Boquerón Member. The middle part of the Boquerón Member is characterized by increasing proportions of *Muricohedbergella* (mainly *Mu. delrioensis*) and *Whiteinella* (mainly *Whiteinella baltica*) (Fig. 8).

4.3. Benthic foraminifera

A total of 53 genera and 69 species of benthic foraminifera have been recorded in the Baños de la Hedionda section (Fig. 9, Table 2). Calcareous taxa dominate the assemblages (up to 93%) except for sample BH-23 in the Capas Blancas Member, where agglutinated forms make up to 52.4% of the assemblage. There are no benthic foraminifera in the black radiolaritic shales nor in the lowermost 10 cm of the Boquerón Member (Fig. 10).

The number of benthic foraminiferal species ranges from 17 to 38 in the Capas Blancas Member, and the Fisher- α diversity index ranges from 5.14 to 14.62 (Fig. 4). Among benthic morphogroups,



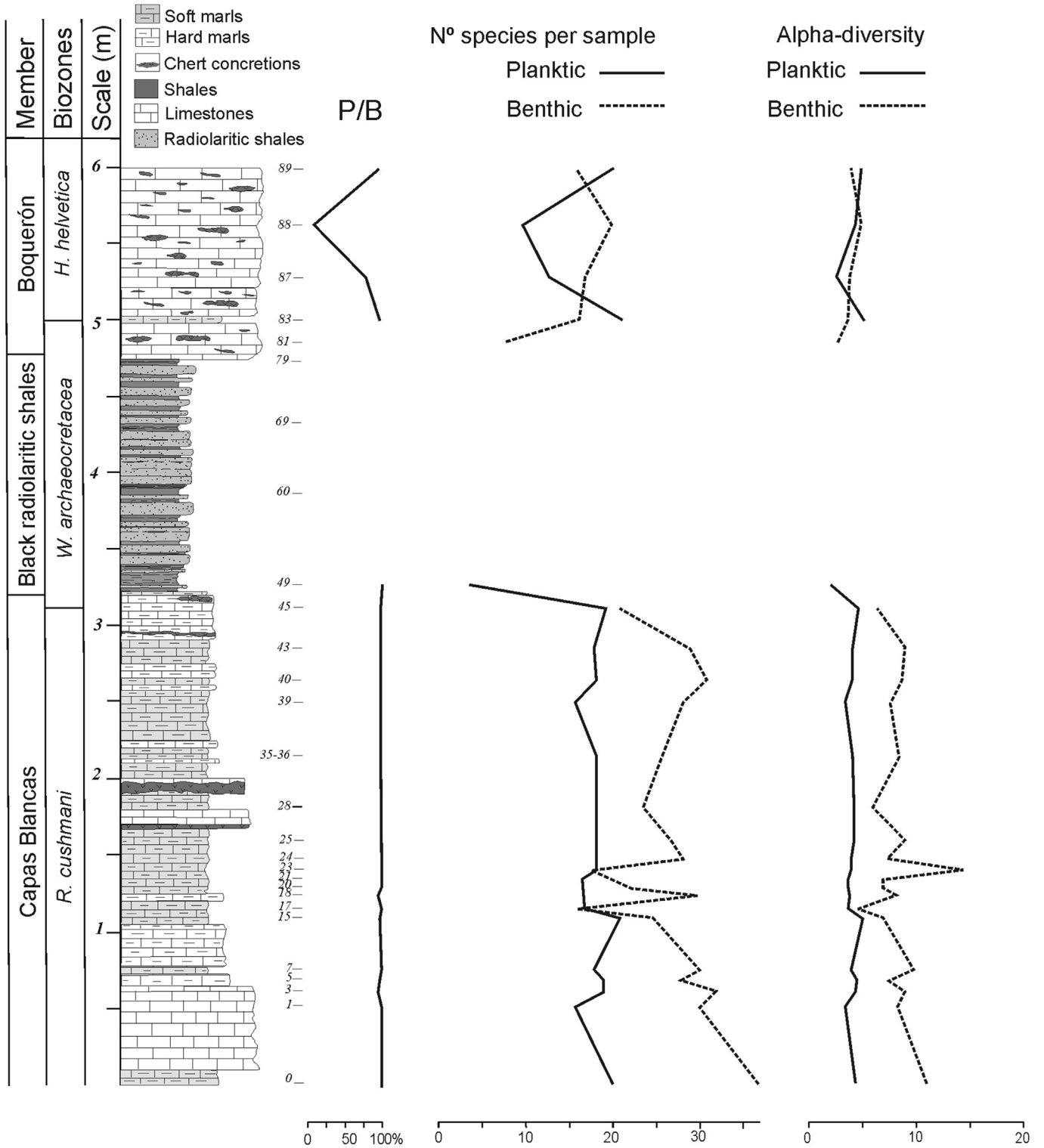


Fig. 4. Stratigraphic distribution of planktic/benthic ratio (P/B) and diversity of planktic and benthic foraminifera.

Fig. 3. Planktic foraminiferal species in the Los Baños de la Hedionda section: A–C, *Rotalipora cushmani* (BH-0). A, umbilical view; B, peripheral view; C, spiral view. D, *Rotalipora cushmani* (BH-0) umbilical view. E, *Rotalipora montsalvensis* (BH-0) umbilical view. F–H, *Whiteinella archaeocretacea* (BH-89). F, umbilical view; G, peripheral view; H, spiral view (note upper half of the test is affected by corrosion by acetic acid after retrieving from indurated rock). I–J, *Whiteinella* cf. *archaeocretacea* (BH-3). I, spiral view; J, umbilical view. K–L, *Praeglobotruncana gibba* (BH-45). K, peripheral view; L, spiral view. M, *Shackoina cenomana* (BH-83) side view. N–P, *Rotalipora greenhornensis* (BH-0). N, spiral view; O, peripheral view; P, umbilical view. Q, *Guembelitra cenomana* (BH-83) side view. R, *Dicarinella* sp. (BH-89) peripheral view. Scale bars: 0.2 mm.

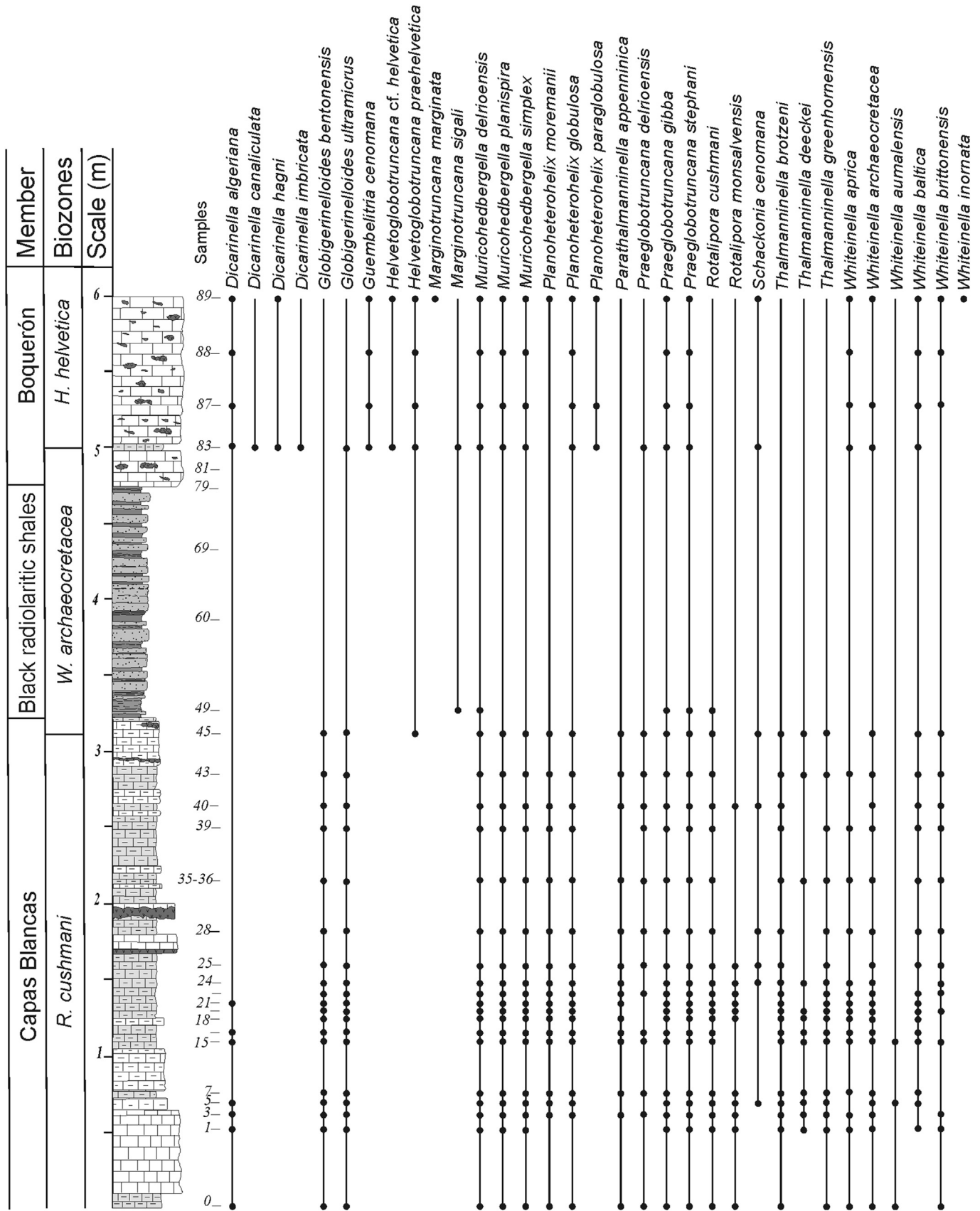


Fig. 5. Stratigraphic distribution of planktic foraminiferal species identified across the upper Cenomanian and lower Turonian at the Baños de la Hedionda section.

Table 1
Count data of planktic foraminifera from the Baños de la Hedionda section.

Sample	Species																														Total specimens				
	<i>Dicarinella algeriana</i>	<i>Dicarinella canaliculata</i>	<i>Dicarinella hagni</i>	<i>Dicarinella imbricata</i>	<i>Globigerinelloides bentonensis</i>	<i>Globigerinelloides ultramicrus</i>	<i>Guembelitra cenomana</i>	<i>Helvetoglobotruncana cf. helvetica</i>	<i>Helvetoglobotruncana praelhelvetica</i>	<i>Marginotruncana marginata</i>	<i>Marginotruncana sigali</i>	<i>Muricohedbergella delrioensis</i>	<i>Muricohedbergella planispira</i>	<i>Muricohedbergella simplex</i>	<i>Parathalminella appenninica</i>	<i>Planoheterohelix globulosa</i>	<i>Planoheterohelix moremani</i>	<i>Planoheterohelix paraglobulosa</i>	<i>Præglobotruncana delrioensis</i>	<i>Præglobotruncana gibba</i>	<i>Præglobotruncana stephani</i>	<i>Rotalipora cushmani</i>	<i>Rotalipora montsalvensis</i>	<i>Schackoia cenomana</i>	<i>Sigalitruncana marianosi</i>	<i>Thalminella brotzeni</i>	<i>Thalminella deeckei</i>	<i>Thalminella greenhornensis</i>	<i>Whiteinella aprica</i>	<i>Whiteinella archaeocretacea</i>	<i>Whiteinella aumalensis</i>	<i>Whiteinella baltica</i>	<i>Whiteinella brittonensis</i>	<i>Whiteinella inornata</i>	
BH-89	50	0	16	0	0	0	3	4	2	17	0	12	30	5	0	12	0	8	0	36	7	0	0	3	1	0	0	0	23	19	0	52	9	3	312
BH-88	3	0	0	0	0	0	1	0	1	0	0	11	0	2	0	1	0	0	0	5	9	0	0	0	0	0	0	0	2	0	0	9	1	0	45
BH-87	115	0	0	0	0	0	10	0	2	0	0	44	30	3	0	5	0	8	0	15	41	0	0	0	0	0	0	4	3	0	29	8	0	317	
BH-83	83	2	12	2	0	10	22	1	25	0	6	19	5	5	0	5	0	7	1	21	33	0	0	4	0	0	0	8	14	0	11	0	0	296	
BH-81	0	0	0	0	0	0	0	0	0	0	0	0	0	0	0	0	0	0	0	0	0	0	0	0	0	0	0	0	0	0	0	0	0	0	0
BH-79	0	0	0	0	0	0	0	0	0	0	0	0	0	0	0	0	0	0	0	0	0	0	0	0	0	0	0	0	0	0	0	0	0	0	0
BH-69	0	0	0	0	0	0	0	0	0	0	0	0	0	0	0	0	0	0	0	0	0	0	0	0	0	0	0	0	0	0	0	0	0	0	0
BH-60	0	0	0	0	0	0	0	0	0	0	0	0	0	0	0	0	0	0	0	0	0	0	0	0	0	0	0	0	0	0	0	0	0	0	0
BH-49	0	0	0	0	0	0	0	0	0	0	4	4	0	0	0	0	0	0	0	2	3	0	0	0	0	0	0	0	0	0	0	0	0	0	13
BH-45	0	0	0	0	14	2	0	0	2	0	0	18	29	21	5	4	3	0	7	47	44	27	0	1	0	57	2	22	0	4	0	2	1	0	312
BH-43	0	0	0	0	17	5	0	0	0	0	0	19	12	20	10	7	7	0	15	13	89	20	0	0	37	3	12	2	4	0	6	13	0	311	
BH-40	0	0	0	0	11	5	0	0	0	0	0	11	36	26	26	8	1	0	4	39	32	44	1	1	0	44	0	2	9	0	20	13	0	333	
BH-39	0	0	0	0	14	3	0	0	0	0	0	12	19	23	0	5	2	0	2	21	110	33	0	0	36	0	16	3	3	0	5	3	0	310	
BH-35-36	0	0	0	0	13	5	0	0	0	0	0	13	21	31	7	9	4	0	10	21	80	33	0	0	48	2	6	2	4	0	12	3	0	324	
BH-28	0	0	0	0	12	3	0	0	0	0	0	16	23	32	5	12	3	0	6	33	64	21	0	1	0	29	0	2	7	8	0	16	2	0	295
BH-25	0	0	0	0	18	7	0	0	0	0	0	14	36	22	8	1	4	0	4	13	58	20	3	1	0	73	0	18	0	3	0	7	5	0	315
BH-24	0	0	0	0	28	2	0	0	0	0	0	31	15	31	2	9	11	0	22	72	26	7	1	0	34	9	8	4	6	0	0	7	0	325	
BH-23	0	0	0	0	19	12	0	0	0	0	0	24	51	8	9	6	1	0	2	40	26	2	2	0	64	0	18	3	15	0	39	4	0	345	
BH-21	2	0	0	0	16	11	0	0	0	0	0	25	23	10	13	15	11	0	0	22	59	4	5	0	68	0	19	7	2	0	36	0	0	348	
BH-20	0	0	0	0	28	4	0	0	0	0	0	10	25	10	0	10	6	0	0	45	51	7	2	0	45	3	24	21	6	0	25	3	0	325	
BH-18	0	0	0	0	10	8	0	0	0	0	0	10	24	25	29	2	1	0	0	47	60	7	4	0	12	4	43	12	8	0	20	0	0	326	
BH-17	0	0	0	0	14	6	0	0	0	0	0	19	30	18	5	1	1	0	4	88	6	0	0	0	86	1	34	4	9	0	20	1	0	347	
BH-15	1	0	0	0	9	6	0	0	0	0	0	7	17	17	9	3	1	0	2	35	61	13	1	0	60	12	13	4	10	3	25	8	0	317	
BH-7	0	0	0	0	23	7	0	0	0	0	0	53	21	20	4	6	2	0	2	43	60	12	4	0	52	4	3	3	13	0	12	0	0	344	
BH-5	20	0	0	0	33	8	0	0	0	0	0	48	15	21	1	8	3	0	0	26	43	15	5	2	0	33	4	8	0	11	5	0	0	314	
BH-3	5	0	0	0	23	7	0	0	0	0	0	44	18	23	1	5	2	0	1	18	39	23	1	0	49	6	14	21	19	0	0	24	0	343	
BH-1	15	0	0	0	16	4	0	0	0	0	0	22	17	39	0	0	0	0	0	27	26	14	16	0	0	27	1	42	59	11	0	3	6	0	345
BH-0	13	0	0	0	19	27	0	0	0	0	0	72	37	33	2	18	6	0	9	34	31	8	17	1	0	44	0	9	16	4	17	0	2	0	419

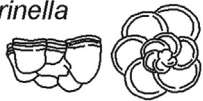




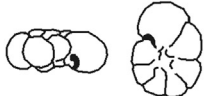

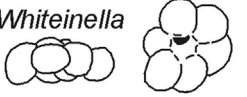



Morphogroup	Genera	Habitat	Strategy	Requirements	
				Oxygenation	Trophic
Strongly keeled trochospiral	<i>Dicarinella</i> 	Intermediate-dweller	Intermediate	Oxygenated	Mesotrophic
	<i>Parathalmanninella</i> <i>Thalmanninella</i> 	Intermediate to deep-dweller	Specialist	Well-oxygenated	Oligotrophic
	<i>Rotalipora</i> 	Intermediate to deep-dweller	Specialist	Well-oxygenated	Oligotrophic
Weakly keeled trochospiral	<i>Helvetoglobotruncana</i> 	Surface-dweller	Intermediate to specialist	Oxygenated to well-oxygenated	Oligotrophic to mesotrophic
	<i>Praeglobotruncana</i> <i>Marginotruncana</i> 	Intermediate-dweller	Intermediate	Oxygenated	Oligotrophic to mesotrophic
Unkeeled trochospiral	<i>Muricohedbergella</i> 	Deep-dweller	Opportunist	Oxygenated to poorly-oxygenated	Eutrophic
	<i>Shackoina</i> 	Intermediate-dweller	Intermediate	Oxygenated to poorly-oxygenated	Mesotrophic to eutrophic
	<i>Whiteinella</i> 	Surface-dweller	Opportunist	Oxygenated to poorly-oxygenated	Mesotrophic to eutrophic
Planispiral	<i>Globigerinelloides</i> 	Surface to intermediate-dweller	Opportunist to intermediate	Oxygenated to poorly-oxygenated	Mesotrophic to eutrophic
Biserial	<i>Planoheterohelix</i> 	Surface to intermediate-dweller	Opportunist	Oxygenated to poorly-oxygenated	Eutrophic
Triserial	<i>Guembelitra</i> 	Surface-dweller	Opportunist	Poorly-oxygenated	Eutrophic

Fig. 6. Planktic foraminiferal morphogroups and inferred life style including redox and trophic requirements.

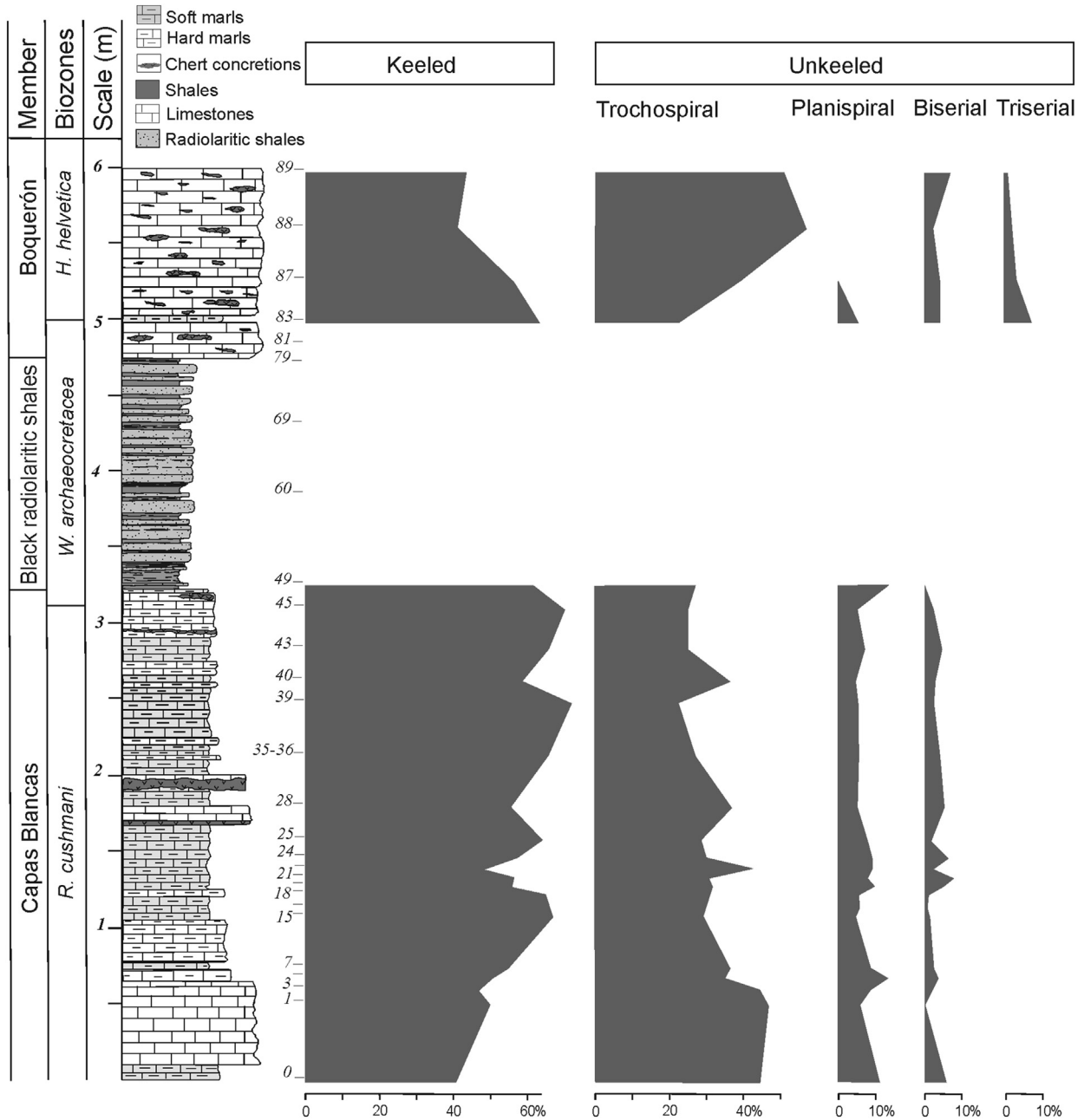


Fig. 7. Stratigraphic distribution of planktic foraminiferal morphogroups.

the biconvex trochospiral (e.g., *Gyroidinoides globosus*, *Charltonina australis*, *Charltonina* sp., *Gavelinella cenomanica* and *Gavelinella* sp.) and cylindrical elongated morphogroups (e.g., *Tritaxia gaultina*, *Laevidentalina* spp., *Praebulimina* spp. and *Marsonella oxycona*) dominate (Fig. 10). Pseudospheric forms such as *Ammosphaeroidina* spp. are also common in the Capas Blancas Member. The epifaunal morphogroups are more abundant than infaunal ones (Fig. 11). A significant increase in the percentages of *Charltonina australis* (17.4%, BH-17), *Gavelinella* spp. (22.8%, BH-17) and *Glomospira* spp. (23.8%, BH-23) has been observed between 1 m and 1.5 m in the Capas Blancas Member (Fig. 10).

Assemblages recorded immediately above the barren interval in the Boquerón Member are significantly different from those in the Capas Blancas Member. The number of species increases from the base (9, sample BH-81) to the top (21, sample BH-88) of the

Boquerón Member, and the Fisher- α index increases from 2.95 to 4.95 (Fig. 4). These values are lower than in the Capas Blancas Member. Assemblages in the Boquerón Member are dominated by biconvex trochospiral (*Gyroidinoides beisseli* and *Gyroidinoides globosus*), cylindrical (*Praebulimina* spp., *Tritaxia gaultina* and *Pleurostomella* spp.) and planoconvex trochospiral morphogroups (*Stensioeina exsculpta*). Infaunal forms are dominant relative to epifaunal ones (Fig. 11, Table 3). The lower part of this member is characterized by high proportions of species that were scarcer in the Capas Blancas Member, such as *Gyroidinoides beisseli* (24.6%), *Praebulimina* spp. (35.0%), *Stensioeina exsculpta* (17.5%), and *Pleurostomella* spp. (5.3%) (Fig. 10). Taxa such as *Tappanina* sp. (21.0%), *Gaudryina* spp., *Gavelinella* spp. and *Lenticulina* spp. are recorded immediately above the lowermost sample of the Boquerón Member (Fig. 10).

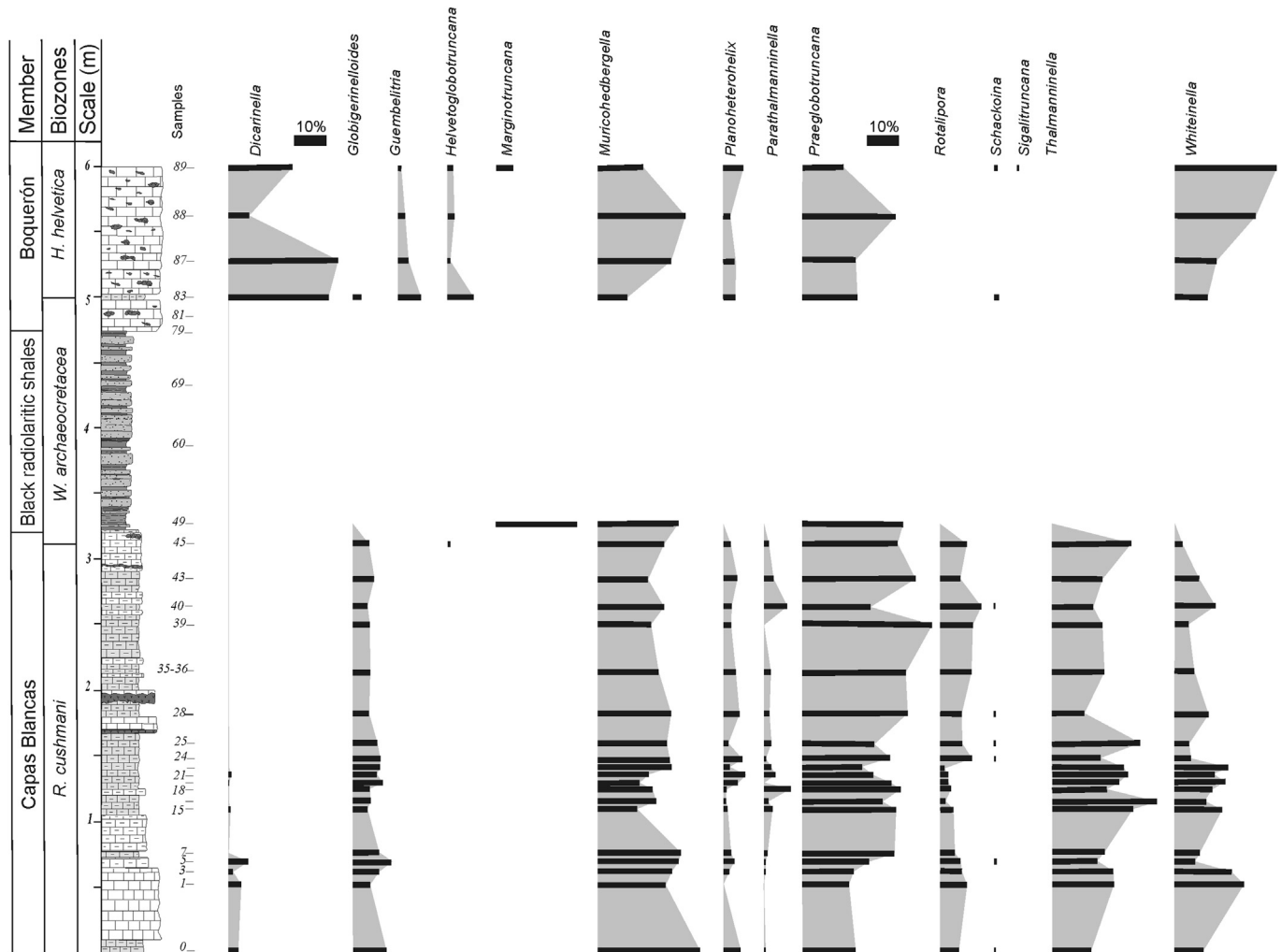


Fig. 8. Percentages of planktic foraminiferal genera across the studied interval.

4.4. Geochemistry

4.4.1. Redox proxies

The analysis of redox proxies allowed us to subdivide the studied section into three intervals that correspond to the three stratigraphic units (Fig. 12): the Capas Blancas Member (*R. cushmani* Biozone), the black radiolaritic shales (*W. archaeocretacea* Biozone), and the Boquerón Member (topmost of *W. archaeocretacea* and base of the *H. helvetica* Biozone).

The Capas Blancas Member (*R. cushmani* Biozone) is characterized by very low values of Cr/Al, U/Th, V/Al, Mo_{EF} , Mo_{aut} , U_{EF} and U_{aut} ratios, followed by a sudden increase in U/Th, V/Al, U_{EF} and U_{aut} ratios in the black radiolaritic shales (*W. archaeocretacea* Biozone), with the highest values recorded in the upper part of the black radiolaritic shales (Fig. 12). A gradual increase in Cr/Al, Mo_{EF} and Mo_{aut} ratios within the black radiolaritic shales leads to the highest values in the upper part of this unit. U_{EF} and Mo_{EF} reach significantly high values in the black radiolaritic shales (7.46 and 22.38, respectively); according to Tribouillard et al. (2012), an elemental enrichment factor >3 is considerable, and >10 is considered as a strong enrichment.

At the base of the Boquerón Member limestones (*H. helvetica* Biozone), the redox ratios decrease down to the original values recorded in the Capas Blancas Member (Fig. 12).

4.4.2. Palaeoproductivity proxies and TOC

The selected palaeoproductivity proxies and TOC show the most significant changes in the black radiolaritic shales (Fig. 13), except for the Ba/Al ratio which shows a prominent peak in the lower part of the Capas Blancas Member (sample BH-7). A peak in the P/Ti ratio has been recorded towards the base of the black radiolaritic shales coincident with a strong decrease in the %CaCO₃ (Fig. 13), which shows very low values in this unit (0.5–3.6 wt.%). The TOC and TS reach the maximum values in the upper part of the black radiolaritic shales (4.8 wt.% and 2.2 wt.%, respectively, sample BH-69), in the same horizon where maximum values in the redox proxies Cr/Al, V/Al, U_{EF} and U_{aut} have been recorded (Figs. 12 and 13). TOC and TS return to lower values and the %CaCO₃ increases at the base of the Boquerón Member (*H. helvetica* Biozone, Fig. 13).

5. Palaeoenvironmental interpretation

5.1. Capas Blancas Member: pre-extinction phase

The Capas Blancas Member is characterized by the dominance of planktic foraminifera indicative of a good water-column tiering, including potential deep-dweller specialists (e.g. *Thalmanninella* and *Rotalipora*) and opportunists (*Muricohedbergella*), intermediate-dwellers (e.g. *Praeglobotruncana*), and potentially surface-dweller opportunists (e.g. *Whiteinella*, *Globigerinelloides*

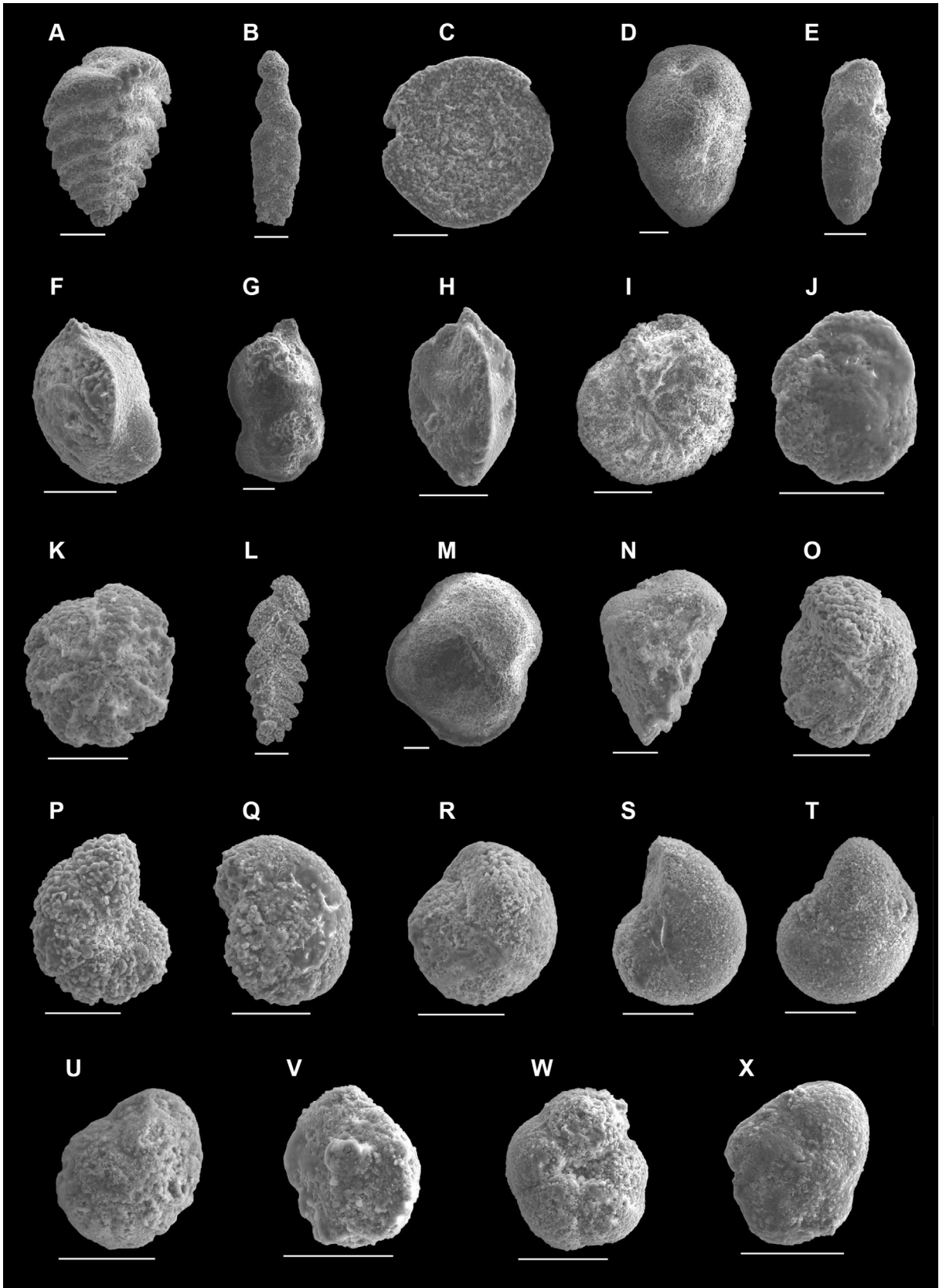


Fig. 9. Benthic foraminiferal species in the Los Baños de la Hedionda section: A, *Spiroplectammina roemeri* (BH-0). B, *Plectina pinswagensis* (BH-0). C, *Ammodiscus* sp. (BH-0). D, *Arenobulimina* sp. (BH-0). E, *Lingulina* sp. (BH-0). F, *Saracenaria* sp. (BH-0). G, *Hemibulimina* sp. (BH-0). H, *Tristix* sp. (BH-0). I, *Stensioeina exsculpta*. J–K, *Charltonina australis* (BH-0). L, *Bolivinopsis spectabilis* (BH-1). M, *Ammosphaeroidina* sp. (BH-1). N, *Gaudryina pyramidata* (BH-3). O–Q, *Gyroidinoides globosus* (BH-18). R, *Gyroidinoides beisseli* (BH-18). S–T, *Valvulinera* sp. (BH-24). U–V, *Globorotalites* sp. (BH-25). W–X, *Gyroidinoides subglobosus* (BH-88). Scale bars: 0.1 mm.

Table 2
Count data of benthic foraminifera from the Baños de la Hedionda section.

Sample	Species																																			
	<i>Ammodiscus</i> spp.	<i>Aragonia</i> sp.	<i>Ammosphaeroidina</i> spp.	<i>Arenobulimina</i> spp.	<i>Astacolus crepidularis</i>	<i>Astacolus gratus</i>	<i>Astacolus</i> spp.	<i>Bathysiphon</i> spp.	<i>Charltonina australis</i>	<i>Charltonina</i> sp.	<i>Clavulinoides</i> sp.	<i>Conorotalites</i> sp.	<i>Coryphostoma</i> spp.	<i>Dorothyia pupa</i>	<i>Dorothyia</i> spp.	<i>Ellipsoidea</i> sp.	<i>Ellipsodimorphina</i> sp.	<i>Epistomina</i> sp.	<i>Epistomina spinulifera</i>	<i>Fronicularia</i> sp.	<i>Gaudryina pyramidata</i>	<i>Gaudryina</i> spp.	<i>Gavelinella cenomanica</i>	<i>Gavelinella</i> spp.	<i>Glandulina</i> sp.	<i>Globorotalites</i> sp.	<i>Globulina</i> sp.	<i>Glomospira</i> spp.	<i>Glomospirella</i> sp.	<i>Gubkinella graysonensis</i>	<i>Gyrogoninoides beisseli</i>	<i>Gyrogoninoides globosus</i>	<i>Gyrogoninoides</i> sp.	<i>Gyrogoninoides subglobosus</i>	<i>Hemibulimina</i> sp.	
BH-89	0	0	0	0	0	0	0	0	0	0	0	0	0	0	0	0	0	0	0	0	3	22	0	5	0	0	0	0	0	0	0	21	17	0	0	0
BH-88	1	0	0	0	0	0	2	0	0	1	0	0	1	0	0	0	0	0	0	0	0	3	0	0	5	0	0	0	1	0	0	51	49	0	3	0
BH-87	0	1	0	0	0	0	3	0	0	0	0	0	0	0	0	0	0	0	0	0	4	4	0	14	0	0	0	0	0	0	22	37	0	0	0	
BH-83	0	0	0	0	0	0	2	0	0	0	0	0	0	0	0	0	0	0	0	0	0	8	0	10	0	0	1	0	0	0	10	65	0	0	0	
BH-81	0	0	0	0	0	0	0	0	0	2	0	0	0	0	0	0	0	0	0	0	0	0	0	0	0	0	0	0	0	0	14	7	0	0	0	
BH-79	0	0	0	0	0	0	0	0	0	0	0	0	0	0	0	0	0	0	0	0	0	0	0	0	0	0	0	0	0	0	0	0	0	0	0	
BH-69	0	0	0	0	0	0	0	0	0	0	0	0	0	0	0	0	0	0	0	0	0	0	0	0	0	0	0	0	0	0	0	0	0	0	0	0
BH-60	0	0	0	0	0	0	0	0	0	0	0	0	0	0	0	0	0	0	0	0	0	0	0	0	0	0	0	0	0	0	0	0	0	0	0	0
BH-49	0	0	0	0	0	0	0	0	0	0	0	0	0	0	0	0	0	0	0	0	0	0	0	0	0	0	0	0	0	0	0	0	0	0	0	0
BH-45	0	0	13	4	1	0	0	0	23	7	3	0	0	0	0	0	0	0	0	0	1	0	2	10	0	0	0	2	0	0	16	36	0	0	0	
BH-43	1	0	16	4	0	0	0	0	3	11	8	0	1	1	0	1	0	0	0	0	2	0	2	0	0	0	1	5	0	0	10	71	0	3	0	
BH-40	0	0	13	8	3	2	1	0	0	32	0	0	1	0	1	0	0	0	0	0	4	0	2	5	0	0	0	2	4	1	8	54	0	3	4	
BH-39	0	0	23	2	0	0	1	0	3	0	4	0	0	0	7	0	0	0	0	0	6	0	6	0	0	0	0	2	0	1	14	75	7	3	2	
BH-35-36	0	0	4	1	0	0	3	0	19	22	0	2	0	0	1	0	0	0	0	0	0	0	3	2	0	0	2	8	0	1	6	26	0	8	1	
BH-28	0	0	26	3	4	4	0	0	12	19	0	0	0	0	2	0	0	0	0	0	1	0	12	8	0	0	0	7	0	0	11	83	0	0	1	
BH-25	1	0	12	2	0	0	0	0	10	0	0	0	0	0	2	0	0	0	0	0	0	0	1	1	0	16	9	3	0	0	4	46	28	0	0	
BH-24	1	0	19	1	0	2	0	0	20	0	0	0	0	0	4	0	0	0	0	0	7	0	13	7	0	16	14	6	0	0	4	63	8	5	0	
BH-23	1	0	0	0	0	0	0	1	0	2	0	0	0	0	0	0	0	0	0	0	0	0	0	0	0	0	10	0	0	0	1	1	1	1	0	
BH-21	0	1	5	1	0	0	0	1	4	0	0	0	0	0	5	0	0	0	0	0	0	0	2	7	0	2	0	10	0	5	5	16	0	0	0	
BH-20	1	0	7	0	0	1	0	0	17	0	0	0	0	2	1	0	0	0	0	0	0	0	2	4	0	16	0	3	0	0	5	57	0	2	0	
BH-18	0	0	14	3	2	1	2	0	14	0	0	2	0	0	15	0	0	0	0	0	3	0	8	7	3	0	0	8	0	9	7	88	0	4	2	
BH-17	0	0	3	2	4	1	0	0	26	0	0	0	0	0	0	0	0	0	0	0	0	0	0	34	0	0	0	1	0	15	20	0	5	0		
BH-15	0	0	8	4	2	0	2	0	20	0	0	0	0	0	0	0	0	0	0	2	0	6	2	0	2	0	5	1	6	63	25	6	0	0		
BH-7	0	0	4	0	1	1	0	0	16	0	0	0	0	0	5	0	2	0	0	0	6	0	2	1	0	2	1	0	3	3	3	61	0	0	0	
BH-5	0	0	10	6	0	0	0	0	8	0	0	0	3	0	3	0	0	0	0	1	12	0	3	11	0	5	6	1	9	0	1	83	0	9	0	
BH-3	0	0	9	4	3	0	1	0	29	0	0	0	0	1	0	0	0	1	0	0	5	1	8	0	0	2	0	7	3	21	75	1	12	0		
BH-1	0	0	10	1	0	0	0	0	24	0	0	0	0	0	0	0	0	0	3	0	9	1	10	7	0	4	6	3	1	7	73	0	3	0		
BH-0	2	0	16	2	3	2	1	0	21	0	0	1	0	0	1	0	0	0	0	0	14	0	16	9	1	0	0	0	1	6	10	72	0	2	2	

Sample	Species																																		
	<i>Hyperammina</i> sp.	<i>Laevidentalina</i> spp.	<i>Lagena</i> sp.	<i>Lenticulina rotulata</i>	<i>Lenticulina</i> spp.	<i>Lenticulina truncata</i>	<i>Lingulina</i> sp.	<i>Marginulina</i> sp.	<i>Marginulinopsis</i> sp.	<i>Marssonella oxycona</i>	<i>Oolina</i> spp.	<i>Patellina</i> sp.	<i>Plectina pinswangensis</i>	<i>Pleurostomella</i> spp.	<i>Præbulimina</i> spp.	<i>Pyrulina</i> spp.	<i>Pyrulinoidea</i> spp.	<i>Quadriformina</i> sp.	<i>Ramulina</i> spp.	<i>Rhabdammina</i> sp.	<i>Saracenaria</i> sp.	<i>Spiroplectammina roemeri</i>	<i>Spiroplectammina</i> sp.	<i>Spiroplectammina spectabilis</i>	<i>Stensioeina exsculpta</i>	<i>Stensioeina granulata</i>	<i>Stensioeina</i> sp.	<i>Tappanina selmensis</i>	<i>Tappanina</i> sp.	<i>Textularia</i> sp.	<i>Tristix</i> sp.	<i>Tritaxia gaultina</i>	<i>Vaginulinopsis</i> sp.	<i>Valvulineria</i> sp.	Total specimens
BH-89	0	8	0	0	9	0	0	0	0	19	0	0	6	8	54	0	1	0	0	0	0	0	0	52	0	0	0	2	0	0	28	0	5	261	
BH-88	0	16	0	0	9	0	0	0	0	12	0	0	0	9	47	2	1	0	0	0	0	0	1	101	0	0	0	1	0	0	27	0	0	343	
BH-87	0	1	0	0	12	0	0	0	0	4	0	0	4	35	43	0	1	0	1	0	0	0	0	59	0	0	0	69	0	0	15	0	0	329	
BH-83	0	8	0	0	7	0	0	0	0	0	0	0	5	7	117	0	8	0	0	0	0	0	0	34	0	0	0	17	2	0	30	0	3	334	
BH-81	0	3	0	0	0	0	0	0	0	0	0	0	0	3	13	0	0	0	0	0	0	0	0	10	0	0	0	0	0	4	0	1	57		
BH-79	0	0	0	0	0	0	0	0	0	0	0	0	0	0	0	0	0	0	0	0	0	0	0	0	0	0	0	0	0	0	0	0	0		
BH-69	0	0	0	0	0	0	0	0	0	0	0	0	0	0	0	0	0	0	0	0	0	0	0	0	0	0	0	0	0	0	0	0	0		
BH-60	0	0	0	0	0	0	0	0	0	0	0	0	0	0	0	0	0	0	0	0	0	0	0	0	0	0	0	0	0	0	0	0	0		
BH-49	0	0	0	0	0	0	0	0	0	0	0	0	0	0	0	0	0	0	0	0	0	0	0	0	0	0	0	0	0	0	0	0	0		
BH-45	0	13	0	6	4	0	0	0	0	11	0	0	0	1	14	1	5	0	0	0	0	2	0	0	0	0	0	0	0	0	15	0	0	190	
BH-43	0	24	0	2	9	4	0	0	0	2	0	0	0	4	13	2	6	0	0	0	2	4	0	11	0	0	0	0	0	20	0	3	246		
BH-40	0	36	0	5	12	4	0	0	0	4	0	0	0	1	16	1	6	6	0	0	0	5	0	20	0	0	0	0	0	48	0	0	313		
BH-39	0	17	0	0	10	0	0	0	0	6	0	0	0	2	19	1	11	3	0	0	1	5	0	12	0	0	0	1	0	61	0	0	306		
BH-35-36	0	15	0	0	7	0	0	0	0	8	0	0	0	0	17	5	7	0	0	0	1	3	0	7	0	0	0	1	0	24	0	0	204		
BH-28	0	36	0	0	20	0	2	0	0	9	0	0	0	0	14	0	11	3	1	0	0	8	0	0	0	0	0	0	42	0	0	341			
BH-25	0	23	0	0	4	0	0	0	0	1	0	0	0	4	10	1	3	0	1	0	0	1	0	5	3	0	0	1	0	10	0	6	211		
BH-24	0	58	0	7	9	0	0	2	0	18	0	0	0	0	17	0	4	0	0	1	1	3	0	0	0	0	0	0	27	2	3	342			
BH-23	1	5	0	1	1	0	0	0	0	2	0	1	0	0	4	1	1	0	0	1	0	3	0	0	0	0	0	0	4	0	0	42			
BH-21	0	12	0	0	6	0	0	0	0	0	0	0	0	7	6	0	9	0	0	0	0	3	0	0	0	3	0	0	20	0	0	130			
BH-20	0	25	0	4	0	0	0	0	0	4	0	0	0	0	6	1	5	0	0	0	0	2	0	9	0	0	0	0	0	17	0	0	194		
BH-18	0	44	0	8	10	0	0	0	0	16	0	0	0	4	3	6	7	0	3	0	0	6	0	5	0	0	0	0	59	0	0	365			
BH-17	0	0	0	4	12	0	0	0	0	8	0	0	0	0	7	0	2	0	0	0	1	0	0	0	0	0	0	0	4	0	0	149			
BH-15	0	40	1	0	4	0	1	0	0	16	0	0	0	0	3	3	12	0	0	0	3	17	0	0	0	0	0	0	45	0	0	299			
BH-7	0	20	0	5	4	0	1	0	0	13	3	0	0	2	4	4	2	0	2	0	1	7	0	26	0	0	0	0	27	0	0	235			
BH-5	0	22	0	6	6	0	0	0	0	12	0	0	0	0	7	2	2	0	3	0	4	8	0	12	0	0	0	0	0	0	315				
BH-3	0	24	0	12	8	0	1	0	0	7	0	0	0	3	13	0	5	4	1	0	2	10	0	30	0	0	1	0	0	32	0	0	341		
BH-1	0	35	0	24	9	0	1	0	0	7	0	0	0	4	10	2	4	0	8	0	3	3	0	11	0	0	1	0	0	37	0	0	323		
BH-0	0	24	0	10	1	0	1	0	1	19	1	0	1	0	18	1	1	0	3	0	4	9	8	21	0	0	0	0	5	2	22	0	0	334	

and *Planoheterohelix*). This assemblage composition indicates oxygenated to poorly oxygenated mesotrophic conditions both in deep and surface-waters (Fig. 14). *Muricoherbergella* and *Planoheterohelix* (*Heterohelix* before Haynes et al., 2015) are the only components of this assemblage that have been interpreted as opportunists related to poorly oxygenated, eutrophic conditions (e.g. Coccioni and Luciani, 2004; Keller and Pardo, 2004a), but they do not dominate the assemblages in the Capas Blancas Member. *Muricoherbergella delrioensis* was originally interpreted as a surface-dweller by Price and Hart (2002) and Coccioni and Luciani (2004) among others, however Ando et al. (2010) proposed a shift to deep environments across the Albian/Cenomanian boundary.

Among planktic assemblages, a gradual increase in the percentage of keeled forms (*Præglobo truncana stephani* and *Rotalipora cushmani*), parallel to a decrease in unkeeled trochospiral forms (*Muricoherbergella delrioensis* and *Whiteinella aprica*) have been recorded in the lower part of the Capas Blancas Member (Fig. 7). This turnover may be related to a lithological change from limestones to marls and marly limestones, and is coeval with an increase in the Ba/Al ratio (Fig. 12), which is a palaeoproductivity

proxy (Reolid and Martínez-Ruiz, 2012). However, the P/Ti ratio, another palaeoproductivity proxy, does not show any significant fluctuations.

Benthic assemblages from the Capas Blancas Member are slightly dominated by epifaunal species (e.g. *Gyrogonidoides globosus* and *Charltonina australis*; Table 3) but also contain some components of shallow (mainly *Laevidentalina* spp., *Ammosphaeroidina* spp., and *Marsonella oxycona*) and deep (*Tritaxia gaultina*) infaunal microhabitats (Fig. 11). This assemblage composition points to low mesotrophic conditions (Dupraz and Strasser, 1999; Jorissen et al., 2007; Reolid et al., 2008b) in the sea-bottom microhabitats because the composition of morphogroups is equilibrated (Fig. 14), except for a few isolated samples where epifaunal forms make up more than 50% of the assemblages. Typical benthic forms indicative of oxygen-poor, eutrophic conditions (such as *Præbulimina*, *Pleurostomella*, *Tappanina*, *Glomospira* and *Gavelinella*; e.g., Koutsoukos et al., 1990; Coccioni et al., 1993; Widmark, 2000; Gebhardt et al., 2010; Reolid et al., 2015) are scarcely represented (Fig. 10). The marly interval of this member, however, contains quantitative peaks in the abundance of *Charltonina australis*, *Gavelinella* spp.,

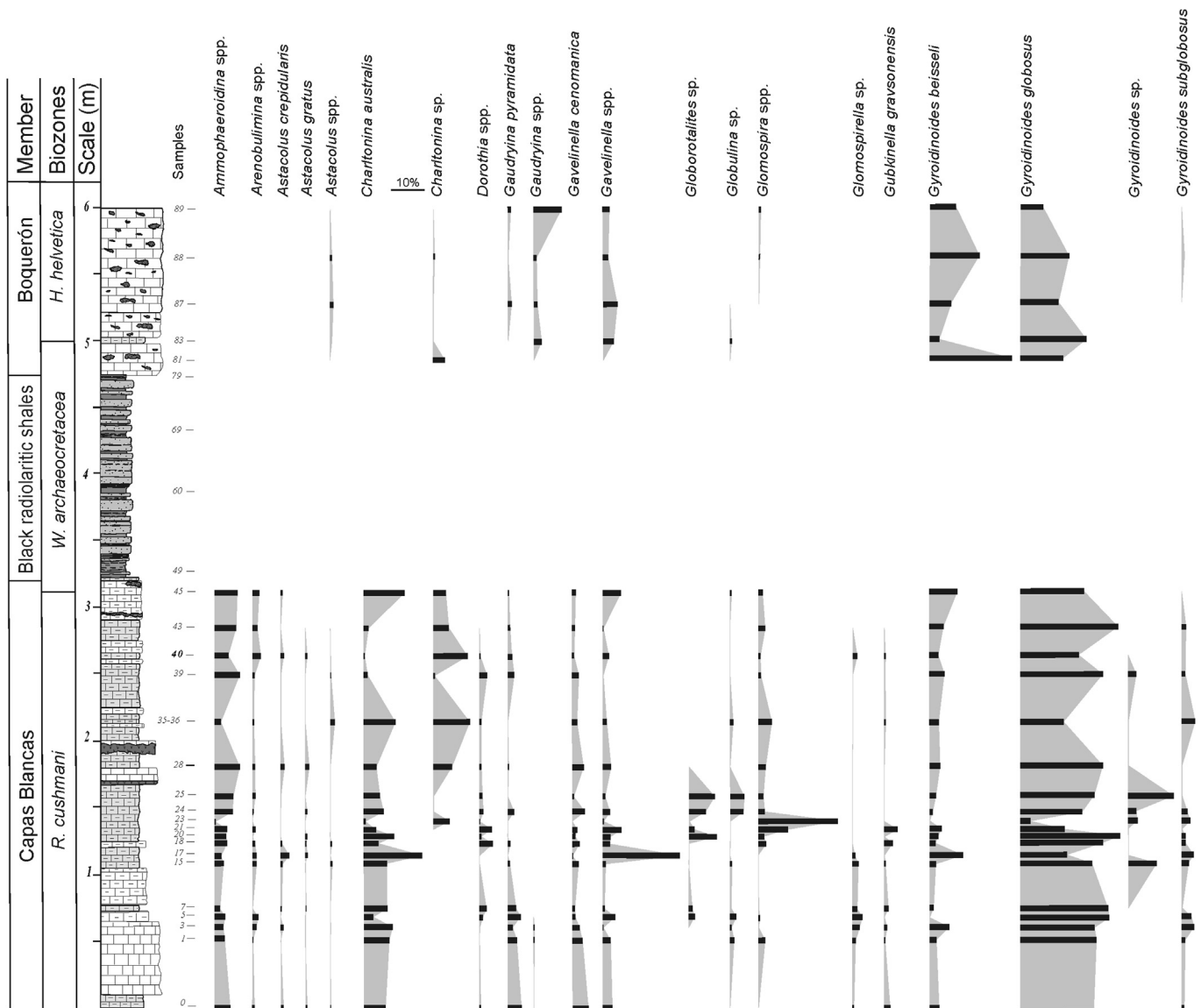


Fig. 10. Stratigraphic distribution of selected benthic foraminiferal species.

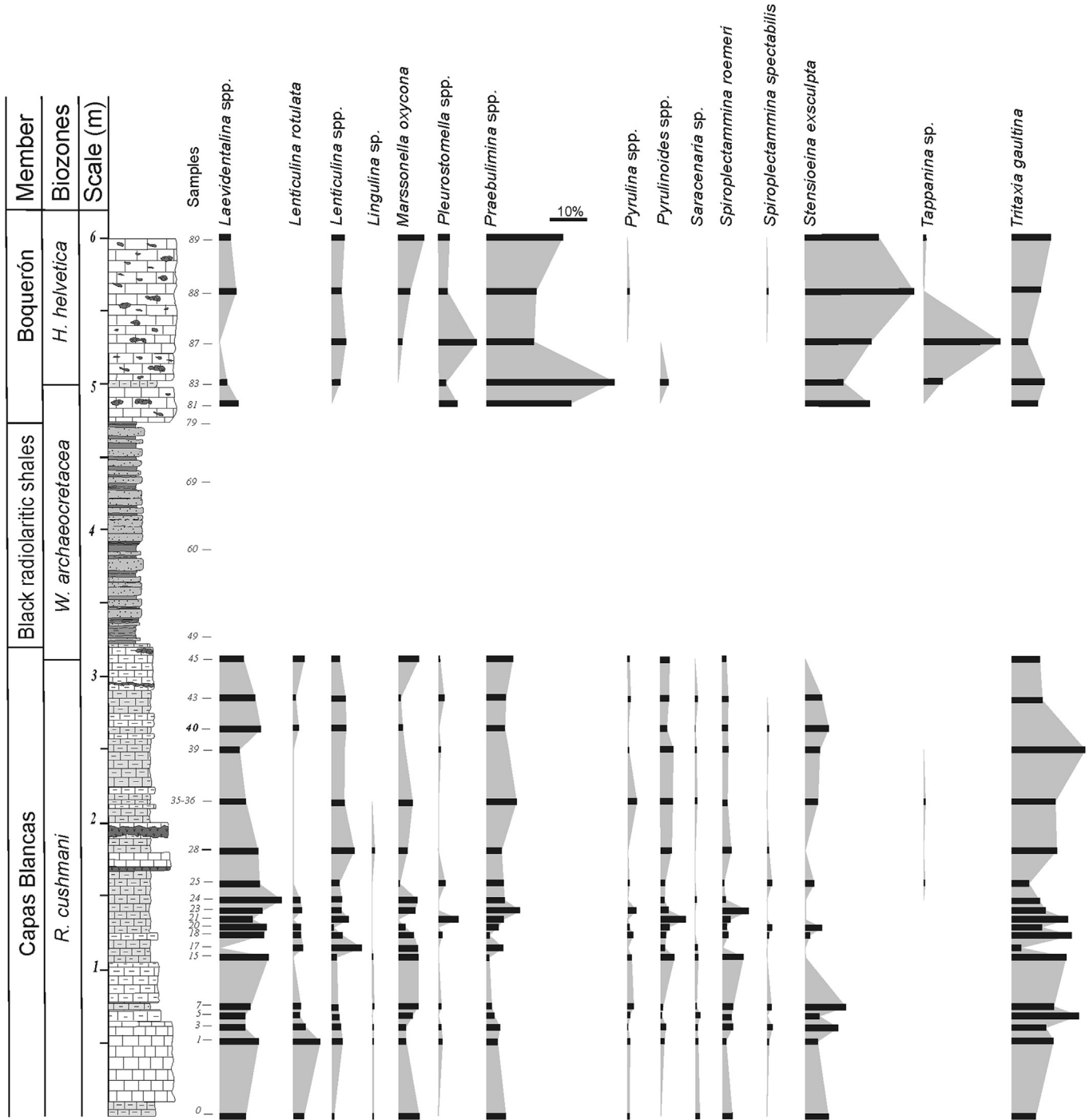


Fig. 10. (continued).

Globorotalites sp., *Pleurostomella* spp. *Spiroplectammina roemeri*, *Glomospira* spp. and *Praebulimina* spp. (samples BH-17 to BH-23), which point to decreased sea-bottom water oxygenation (Fig. 14) (e.g. Gebhardt et al., 2010; Reolid et al., 2015). *Gavelinella* has been interpreted in the literature as a low-oxygen tolerant genus (Sliter, 1975; Koutsoukos et al., 1990; Gertsch et al., 2010), and it occurs in shales with a high concentration of organic matter (Holbourn et al., 2001). *Globorotalites* peaked in abundance under stressful conditions after the Cretaceous/Paleogene impact event (Alegret, 2007; Alegret et al., 2012). The interpretation of dysoxic conditions is supported by a small peak in the U_{EF} values (Fig. 12). This minor

event within the *R. cushmani* Biozone reflects an ecological replacement of opportunistic taxa, with *Gavelinella* as the first colonizer and *Glomospira* and *Praebulimina* as the last ones reaching maximum percentage peaks (Fig. 10).

An increase in the percentage of *Charltonina*, *Glomospira*, *Lenticulina* and *Praebulimina* is recorded immediately above the short interval of dysoxic sea-bottom water conditions (Fig. 10). These genera are not dominant but point to unfavourable conditions in spite of the fact that redox and palaeoproductivity proxies do not change significantly (Figs. 12 and 13). The proliferation of opportunistic forms prior to an anoxic event (and associated variations in

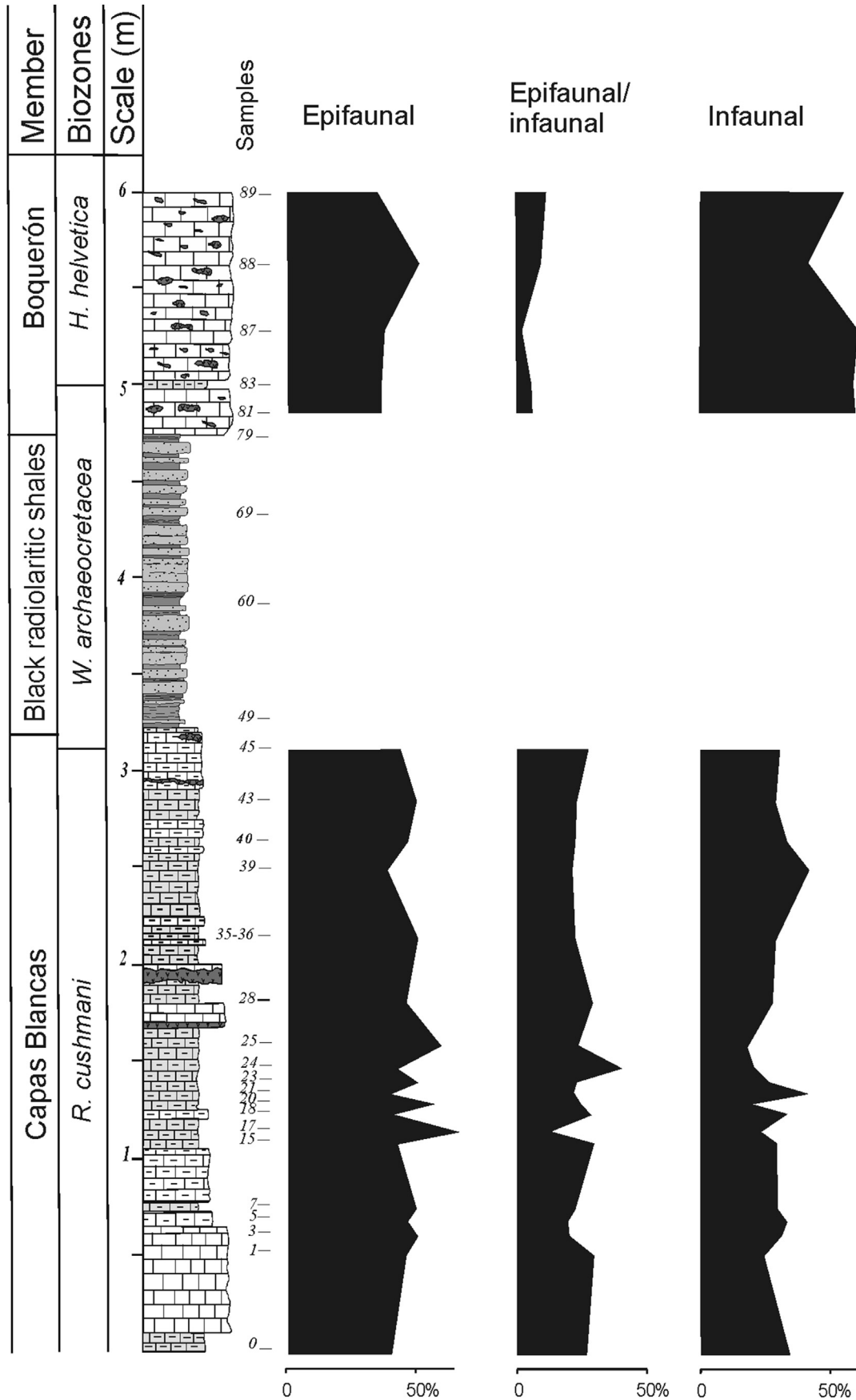


Fig. 11. Relative abundance of benthic foraminiferal inferred microhabitats across the studied interval.

Table 3

Differentiation of morphogroups according to test shape, and inferred life style compared with previous interpretations (Koutsoukos et al., 1990; Hart, 1996; Bak et al., 1997). Note: Koutsoukos et al. (1990) for assemblages from oxygen depleted environments across the Cenomanian/Turonian boundary.

Species	Morphogroup	Subgroup	Chambers	Test form	Life position	Hart (1996)	Koutsoukos et al. (1990)	Bak et al. (1997)
<i>Ammodiscus</i> spp.	B	B2	Multilocular	Coiled flatened	Epifaunal		Epifaunal	Epifaunal
<i>Aragonia</i> sp.				Flatened tapered	Infaunal			
<i>Ammosphaeroidina</i> spp.	B	B1?	Multilocular	Globular	Epifaunal/ Infaunal			
<i>Arenobulimina</i> sp.	C	C1	Multilocular	Elongate	Infaunal	Infaunal		
<i>Astacolus crepidularis</i>				Flatened tapered	Infaunal			
<i>Astacolus gratus</i>				Flatened tapered	Infaunal			
<i>Astacolus</i> spp.				Flatened tapered	Infaunal			
<i>Bathysiphon</i> spp.	A	A	Unilocular	Tubular	Epifaunal			Epifaunal
<i>Charltonina australis</i>				Biconvex trochospiral	Epifaunal			
<i>Charltonina</i> sp.				Biconvex trochospiral	Epifaunal			
<i>Clavulinoides</i> sp.	C	C1	Multilocular	Elongate	Infaunal			
<i>Conorotalites</i> sp.				Planoconvex trochospiral	Epifaunal			
<i>Coryphostoma</i> spp.				Flatened tapered	Infaunal		Infaunal	
<i>Dorothia pupa</i>	C	C1	Multilocular	Elongate	Infaunal		Infaunal	Shallow to deep infaunal
<i>Dorothia</i> spp.	C	C1	Multilocular	Elongate	Infaunal		Infaunal	Shallow to deep infaunal
<i>Ellipsoidella</i> sp.				Cylindrical tapered	Infaunal		Infaunal	
<i>Ellipsopolymorphina</i> sp.				Cylindrical tapered	Infaunal		Infaunal	
<i>Epistomina</i> sp.				Biconvex trochospiral	Epifaunal			
<i>Epistomina spinulifera</i>				Biconvex trochospiral	Epifaunal			
<i>Frondicularia</i> sp.				Palmate	Epifaunal		Epifaunal/Shallow infaunal	
<i>Gaudryina pyramidata</i>	C	C1	Multilocular	Elongate	Infaunal			
<i>Gaudryina</i> spp.	C	C1	Multilocular	Elongate	Infaunal			
<i>Gavelinella cenomanica</i>				Biconvex trochospiral	Epifaunal	Epifaunal/ infaunal	Epifaunal	
<i>Gavelinella</i> spp.				Biconvex trochospiral	Epifaunal	Epifaunal/ infaunal	Epifaunal	
<i>Glandulina</i> sp.				Cylindrical tapered	Infaunal		Infaunal	
<i>Globorotalites</i> sp.				Planoconvex trochospiral	Epifaunal			
<i>Globulina</i> sp.				Spherical/Globose	Infaunal		Epifaunal/Shallow infaunal	
<i>Glomospira</i> spp.	B	B2	Multilocular	Coiled flatened and streptospiral	Epifaunal		Epifaunal	Epifaunal
<i>Glomospirella</i> sp.	B	B2	Multilocular	Coiled flatened and streptospiral	Epifaunal		Epifaunal	
<i>Gubkinella graysonensis</i>				Spherical/Globose	Infaunal			
<i>Gyroidinoides beisseli</i>				Biconvex trochospiral	Infaunal			
<i>Gyroidinoides globosus</i>				Rounded trochospiral	Epifaunal			
<i>Gyroidinoides</i> sp.				Planoconvex trochospiral	Epifaunal			
<i>Gyroidinoides subglobosus</i>				Planoconvex trochospiral	Epifaunal			
<i>Hemirobulina</i> sp.				Cylindrical tapered	Infaunal			
<i>Laevidentalina</i> spp.				Cylindrical tapered	Infaunal		Epifaunal/Shallow infaunal	
<i>Lagena</i> sp.				Spherical/Globose	Infaunal			
<i>Lenticulina rotulata</i>				Biconvex planispiral	Epifaunal	Epifaunal/ infaunal	Epifaunal	
<i>Lenticulina</i> sp.				Biconvex planispiral	Epifaunal		Epifaunal	
<i>Lenticulina truncata</i>				Biconvex planispiral	Epifaunal			
<i>Lingulina</i> sp.				Flatened tapered	Infaunal		Epifaunal/Shallow infaunal	
<i>Marginulinopsis</i> sp.				Cylindrical tapered	Infaunal			
<i>Marssonella oxycona</i>	C	C1	Multilocular	Elongate	Infaunal	Epifaunal/ infaunal	Infaunal	
<i>Oolina</i> spp.				Spherical/Globose	Infaunal			
<i>Plectina pinswangensis</i>	C	C1	Multilocular	Elongate	Infaunal			
<i>Pleurostomella</i> spp.				Cylindrical tapered	Infaunal		Infaunal	
<i>Praebulimina</i> spp.				Cylindrical tapered	Infaunal		Epifaunal/Shallow infaunal	
<i>Pyrulina</i> spp.				Cylindrical tapered	Infaunal		Epifaunal/Shallow infaunal	
<i>Pyrulinoides</i> spp.				Cylindrical tapered	Infaunal		Epifaunal/Shallow infaunal	
<i>Quadriformina</i> sp.				Biconvex trochospiral	Epifaunal		Epifaunal	
				Tubular or branching	Epifaunal			

(continued on next page)

Table 3 (continued)

Species	Morphogroup	Subgroup	Chambers	Test form	Life position	Hart (1996)	Koutsoukos et al. (1990)	Bak et al. (1997)
<i>Ramulina</i> spp.				Tubular or branching	Epifaunal		Epifaunal	
<i>Saracenaria</i> sp.				Triangular elongate	Infaunal			
<i>Spiroplectammina romeri</i>	C	C1	Multilocular	Elongate	Infaunal			Shallow to deep infaunal
<i>Spiroplectammina</i> sp.	C	C1	Multilocular	Elongate	Infaunal			
<i>Stensioeina exsculpta</i>				Planoconvex trochospiral	Epifaunal			
<i>Stensioeina granulata</i>				Planoconvex trochospiral	Epifaunal			
<i>Tappanina selmensis</i>				Flattened tapered	Infaunal			
<i>Textularia</i> sp.	C	C1	Multilocular	Elongate	Infaunal		Infaunal	
<i>Tritaxia gaultina</i>	C	C1	Multilocular	Elongate	Infaunal		Infaunal	
<i>Vaginulinopsis</i> sp.				Flattened tapered	Infaunal			
<i>Valvulineria</i> sp.				Planoconvex trochospiral	Epifaunal	Infaunal	Epifaunal	

geochemical proxies) was also documented across the Toarcian Oceanic Anoxic Event by Reolid et al. (2012a). A significant decrease in the diversity of benthic foraminifera occurs towards the top of the Capas Blancas Member, and is congruent with the progress of the unfavourable conditions at the seafloor.

Ichnofabric analysis carried out by Rodríguez-Tovar et al. (2009a) revealed the occurrence of *Chondrites*, *Planolites*, *Trichichnus* and *Palaeophycus* at the top of the Capas Blancas Member. These authors interpreted a well-oxygenated environment punctuated by short intervals of oxygen-depleted conditions.

5.2. Black radiolaritic shales: Oceanic Anoxic Event 2

The lack of benthic foraminifera in the black radiolaritic shales

and the occurrence of planktic foraminifera only in the lowermost sample (BH-49) point to adverse conditions during sedimentation of the black shales. Low-diversity planktic assemblages from sample BH-49 (Fig. 4) are characterized by opportunist taxa from relatively deep waters (*Muricohedbergella delrioensis*, Fig. 6), which indicate poorly oxygenated waters and eutrophic conditions (Fig. 14). Non-opportunist intermediate-dwellers (*Praeglobotruncana*) and abundant *Marginotruncana* (K-strategists; Petrizzo, 2002) have also been identified in this sample, whereas no deep-dweller specialists such as *Rotalipora* and *Thalmaninella* have been observed. The fact that *Marginotruncana sigali* first occurred in the lower part of the black radiolaritic shales is difficult to interpret. We argue that this species, which was considered as a specialist taxon by Petrizzo (2002), may have been adapted to oxygen-

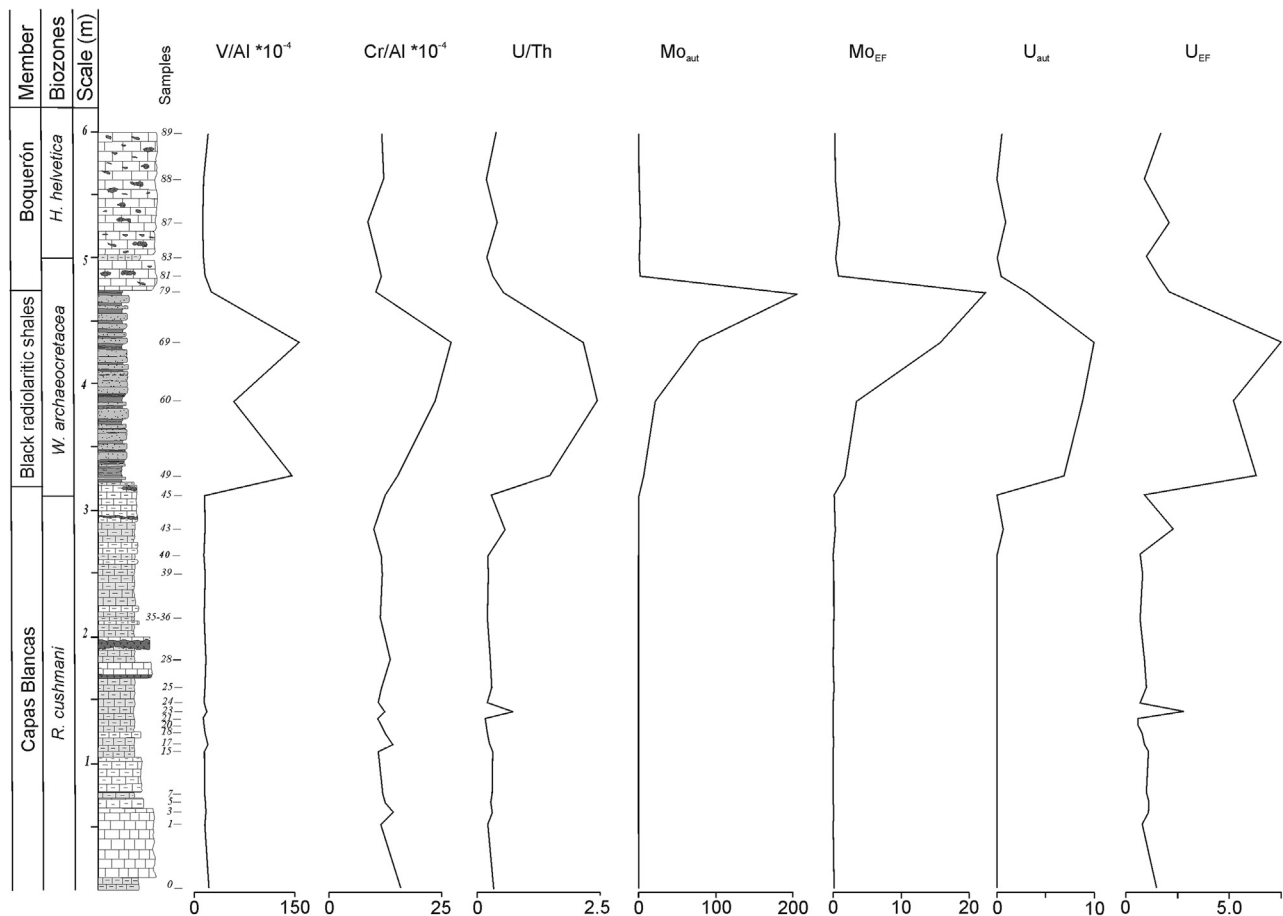


Fig. 12. Stratigraphic fluctuations of geochemical redox proxies and U- and Mo-based proxies (enrichment factor and authigenic content).

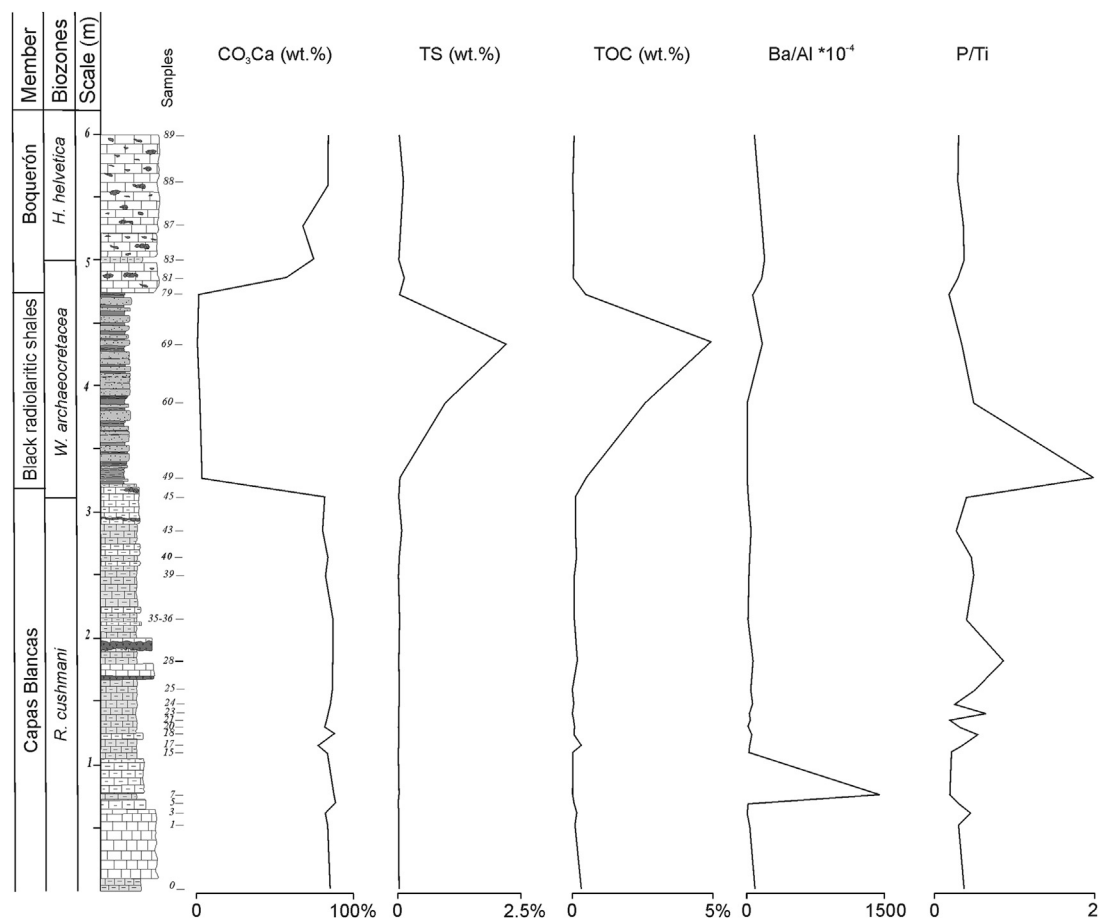


Fig. 13. Stratigraphic distribution of %CaCO₃, total sulphur (TS), total organic carbon (TOC), and geochemical palaeoproductivity proxies (Ba/Al and P/Ti ratios).

restricted conditions. Except for sample BH-49, the black radiolaritic shales are barren of foraminifera, suggesting adverse conditions in the water column. According to Huber et al. (1999), increased pCO₂ and deep water warming may have caused a breakdown in the vertical tiering of the water column, accounting for the extinction of specialist deeper-dwelling species. Alternatively, increased bottom water ocean acidification might explain the loss of benthic foraminiferal tests and post-depositional loss of planktic tests.

Redox conditions in the water column and at the seafloor may be inferred from the analysis of redox-sensitive trace elements (Cr, Mo, U and V), which tend to co-precipitate with sulfides (mainly pyrite) and are usually not remobilized during diagenesis in the absence of post-depositional replacement of oxidizing agents (Tribouillard et al., 2006). The enhancement in redox sensitive elements (Cr/Al, V/Al, U/Th, Mo_{EF}, Mo_{aut}, U_{EF} and U_{aut}) points to depleted oxygen conditions during deposition of the black radiolaritic shales (Figs. 12 and 14). U-based proxies (U_{EF} = 7.46 and U_{aut} = 10.07) and increased TOC values (4.84 wt.%) point to depleted oxygen conditions in the lower part of the water column (Fig. 14).

The P/Ti ratio is a commonly used proxy for productivity (Latimer and Filippelli, 2001; Robertson and Filippelli, 2008; Reolid et al., 2012a,b, 2015). Increased values are related to a higher phosphorous supply to the seafloor derived from biological processes, not from terrigenous components (Latimer and Filippelli, 2001; Flores et al., 2005; Sen et al., 2008). At Baños de la Hedionda section, the increase in P/Ti values at the base of the *W. archaeocretacea* Biozone indicates an abrupt increase in

productivity (Fig. 13). Such an increase in the P/Ti ratio was also identified at the base of the *W. archaeocretacea* biozone in the Tunisian Oued Bahloul section (Reolid et al., 2015). Mort et al. (2007a) suggested that the increase in P-accumulation rates coinciding with OAE2 may be related to an overall increase in surface-water productivity. However, maximum values of P/Ti ratio do not coincide with maximum values of TOC or U_{EF} in Baños de la Hedionda section (Figs. 12 and 13). The Ba/Al ratio, which has also been used as a palaeoproductivity proxy (Sun et al., 2008; Reolid and Martínez-Ruiz, 2012; Reolid et al., 2012a,b), does not show any significant fluctuations in the black shales interval.

The initial increase in opportunist planktic foraminifera typical of poorly oxygenated environments and eutrophic conditions, and the disappearance of deep-dweller specialists (e.g. *Rotalipora*) and benthic foraminifera coincide with the onset of the OAE2 as well as with the high P/Ti values. Persistent oxygen restricted conditions are confirmed by the relatively higher TOC values (reaching 4.84 wt.%), which point to higher accumulation of organic matter derived from surface primary productivity than in the Capas Blancas Member (Schlanger and Jenkyns, 1976; Arthur et al., 1990; Ingall et al., 1993; Van Cappellen and Ingall, 1994; Mort et al., 2007a). TOC values have been used as an indirect palaeoproductivity proxy when TOC is related to phytodetritus associated with phytoplankton or dinoflagellate remains (e.g., Calvert and Fontugne, 2001; Gupta and Kawahata, 2006; Plewa et al., 2006; Su et al., 2008). According to Tribouillard et al. (2006), the TOC is generally proportional to surface-water productivity and constitutes a useful palaeoproductivity proxy in spite of certain complications attributable to efficient organic recycling, export

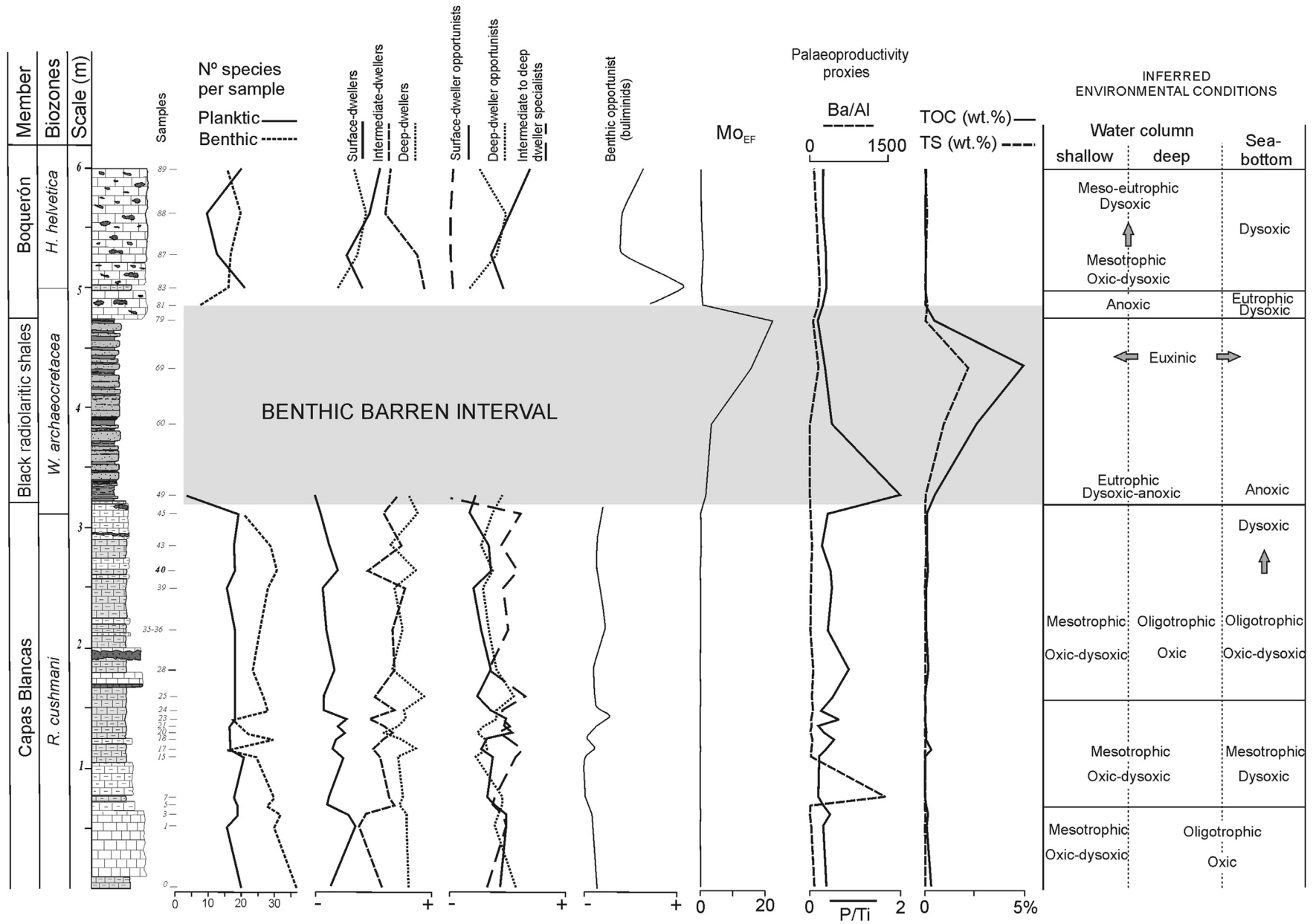


Fig. 14. Evolution of trophic conditions, productivity and oxygenation in the water column and at the seafloor (sea-bottom waters) inferred from foraminiferal assemblages and geochemical proxies. Note according to Fig. 5: surface-dweller opportunists include *Globigerinelloides*, *Planoheterohelix*, *Guembeltria*, *Planoheterohelix* and *Whiteinella*; deep-dweller opportunists include *Muricohedbergella* (mainly *Mu. delrioensis*); and intermediate and deep-dweller specialists include *Parathalmanninella*, *Rotalipora* and *Thalmanninella*.

productivity, delivery to the sediment–water interface and final burial. High TOC values, however, may also result from low bottom-water ventilation and oxygen depletion, and are not necessarily related to high surface productivity.

Radiolarians are a major component of the black radiolaritic shales (Fig. 2d) and indicate abnormally high surface productivity. High concentrations of radiolarians have been typically documented from black shales related to OAE2 in northern European sections (e.g., Jarvis et al., 1988; Scopelliti et al., 2004; Kędzierski et al., 2012; Uchman et al., 2013), which are often barren of planktic foraminifera. According to Jarvis et al. (1988), major changes in oceanic circulation during the C–T transition enhanced upwelling currents, with nutrient-rich deep-waters emerging towards the surface. Moreover, abundance of radiolarians in the same sediments is consistent with shallowing of the oxygen–minimum zone caused by enhanced ocean–surface productivity.

In Recent marine environments there is a positive correlation between TOC and total sulphur (TS) mainly coming from pyrite (Berner and Raiswell, 1983). Under depleted oxygen conditions (dysoxic or anoxic), organic matter decays at the seafloor or in the sediment–water interface, resulting in increased reduction rates of sulphate, increased H₂S in the sediment pore-water, and the progressive shallowing of the redox boundary within the sediment. The H₂S reacts with the detritic Fe and forms pyrite. In this sense, the TS in the black shales interval is congruent with the highest TOC values and the oxygenation decrease indicated by V/Al and Cr/Al ratios (Figs. 12 and 13). Maximum values of TOC and redox proxies do not coincide with the maximum peak in P/Ti, which is recorded towards the base of the black radiolaritic shale interval. This might suggest that, in addition to high surface productivity, oxygen depleted conditions across OAE2 may have been exacerbated by other factors, as previously suggested by Mort et al. (2007b).

High Mo_{EF} and Mo_{aut} values require the presence of H₂S (euxinic conditions) (Tribouillard et al., 2012; Zhou et al., 2012). The increase in Mo_{EF} and Mo_{aut} across the black shales indicates a decrease in oxygen availability towards euxinia (Fig. 14). Other authors have reported euxinic conditions from OAE2 (e.g., Wang et al., 2001; Scopelliti et al., 2004; Reolid et al., 2015). Progressively oxygen-depleted conditions from the base of the black shales upwards are compatible with the disappearance of planktic foraminifera, including opportunistic taxa that flourished at the beginning of the eutrophic conditions (e.g., *Muricohedbergella*; BH-49). Alternatively, increased bottom water ocean acidification may account for the loss of the planktic foraminiferal tests.

Marine anoxia during OAE2 is thought to have been related to enhanced biological productivity (e.g. Monteiro et al., 2012; Pogge von Strandmann et al., 2013). Uranium and organic matter in the sediment are related, as uranium may form a complex that dissolves fulvic acid in hemipelagic sediments (Nagao and Nakashima, 1992). In this sense, high values for U_{EF} and U_{aut} are congruent with the high values of TOC. In open-ocean systems with suboxic bottom waters, U_{aut} enrichment is greater than that of Mo_{aut} because U_{aut} accumulation begins at the Fe (II)–Fe (III) redox boundary (Zhou et al., 2012), while Mo_{aut} accumulation becomes more relevant as waters become euxinic. Higher values of U_{aut} recorded in the lower part of the black shale interval are congruent with anoxic conditions not only at the sea-bottom waters but also in the deeper layers of the water column, where deep dwellers such as *Rotalipora* inhabited. However, the upper part of the black shales (BH-69 to BH-79) presents higher values of Mo_{aut} than U_{aut} and indicates euxinic conditions.

Based on ichnologic analyses, Rodríguez-Tovar et al. (2009a) interpreted anoxic conditions during deposition of the black radiolaritic shales in this section, with interruptions by short dysaerobic to oxic periods as suggested by the occurrence of such ichnotaxa

as *Chondrites*, *Planolites*, *Thalassinoides* and rare *Zoophycos* in greenish or light grey silicified shales.

5.3. Boquerón Member: recovery

Foraminiferal assemblages from the Boquerón Member significantly differ from those recorded before OAE2. The lowermost sample of the Boquerón Member only contains benthic foraminifera, while planktic foraminifera reappear 26 cm above the base of this member (including the first occurrence of *Dicarinella* species, namely *D. canaliculata*, *D. hagni* and *D. imbricata*). *Dicarinella algeriana*, a species that has not been recorded in the upper part of the Capas Blancas Member, dominates the assemblages in the lowermost part of the *H. helvetica* Biozone (Fig. 8). The genus *Dicarinella* has been interpreted as an intermediate-dweller typical of oxygenated mesotrophic environments (Coccioni and Luciani, 2004; Fig. 6). Recent studies indicate that *Dicarinella* occupied a slightly deeper habitat than surface-dwellers such as *Helvetoglobotruncana* and *Whiteinella* (MacLeod et al., 2013; Wendler et al., 2013; Huber and Petrizzo, 2014). Planktic assemblages also contain common intermediate to deep-dweller forms such as *Praeglobotruncana*, typical of oxygenated, mesotrophic environments. Opportunist surface-dweller forms indicative of oxygenated to poorly oxygenated waters and mesotrophic to eutrophic conditions are also recorded (e.g., *Whiteinella*, *Guembelitria* and *Planoheterohelix*). The opportunistic surface-dweller *Whiteinella* progressively proliferated during the *H. helvetica* Biozone. *Guembelitria* has been interpreted as an opportunist surface-dweller adapted to poorly oxygenated, eutrophic waters (Coccioni and Luciani, 2004; Reolid et al., 2015) or to variable salinity and nutrient levels (Keller and Pardo, 2004a,b). The deep-dweller specialist *Rotalipora* and the intermediate to deep-dweller specialist *Parathalmanninella* went extinct, and there are no genera occupying this ecologic niche (Fig. 8). Deep-dwellers are represented only by the opportunist genus *Muricohedbergella*, mainly *Mu. delrioensis*, which has also been documented from oxygen-deficient environments (Coxall et al., 2007; Ando et al., 2010). *Guembelitria*, *Mu. delrioensis* and *Planoheterohelix* have been reported as indicators of poorly oxygenated eutrophic conditions (Reolid et al., 2015), but in the studied section also co-occur with diverse planktic assemblages typical of oligotrophic, well-oxygenated mixed layers. Therefore, the presence of these taxa may indicate low oxygenated conditions but not so restricted as during the black radiolaritic shales.

Benthic foraminiferal assemblages are less diverse than in the Capas Blancas Member. They are dominated by opportunistic species of the genera *Praebulimina*, *Gyroidinoides*, *Tappanina* and *Pleurostomella* (e.g., Peryt and Lamolda, 1996). The clear dominance of *Praebulimina* spp. immediately above the extinction interval suggests that they may have behaved as disaster species (Peryt and Lamolda, 1996; Reolid et al., 2015). Buliminids are considered to be indicators of high-food and/or low oxygenation at the seafloor in the modern oceans (e.g., Fontanier et al., 2002; Gooday, 2003). Some species of *Gyroidinoides* have been interpreted as opportunists (e.g. Peryt and Lamolda, 1996). Species of *Praebulimina*, *Pleurostomella* and *Tappanina* have been reported from dysoxic facies in highly eutrophic environments and high organic-matter fluxes (e.g. Eicher and Worstell, 1970; Coccioni et al., 1993; Widmark, 2000; Gustafsson et al., 2003; Gebhardt et al., 2004; Friedrich and Erbacher, 2006; Friedrich et al., 2009; Reolid et al., 2015). Moreover, the dominance of infaunal taxa in the Boquerón Member supports the interpretation of eutrophic and low oxygen conditions at the seafloor (Jorissen et al., 1995). Similarly, dysoxic conditions have also been inferred from infaunal-dominated assemblages immediately above the OAE2 event in the Spanish Menoyo section

(Peryt and Lamolda, 1996).

In contrast, redox proxies do not indicate oxygen depleted conditions in the Boquerón Member. We conclude that the palaeoenvironmental perturbation related to the OAE2 (recorded in the foraminiferal-barren interval of the black radiolaritic shales) induced slow recovery of the foraminiferal assemblages, especially affecting benthic foraminifera, which display low diversity and are dominated by opportunistic species. Detailed analysis of the benthic assemblages shows a succession of abundance peaks that represent the first stages of seafloor recolonization after the OAE2, which correspond to the ecological replacement of mainly opportunistic foraminifera (abundance peaks of *Gyroidinoides beisseli* and *Stensioeina exsculpta* in BH-81, followed by peaks of *Praebulimina* sp. and *Gyroidinoides globosus* in BH-83, and *Tappanina* and *Pleurostomella* in BH-87). The first colonizers were epifaunal forms, and these were followed by abundance peaks of infaunal opportunists, indicating the persistence of adverse conditions at the seafloor.

The first stages of seafloor recolonization by benthic foraminifera occurred prior to water column colonization by planktic forms, mainly by intermediate to deep-dwellers typical of mesotrophic to oligotrophic waters (*Dicarinella algeriana*, *Praeglobotruncana stephani*, *P. gibba*). These data indicate that the recovery of environmental conditions began at the sea-bottom and in the deep and intermediate waters. The subsequent proliferation of surface-dweller opportunists (*Whiteinella baltica*) and deep-dweller opportunists (*Muricohedbergella delrioensis*) adapted to mesotrophic to eutrophic conditions, and the decrease in planktic foraminiferal diversity may indicate the return to poorly oxygenated conditions in the water column during the *H. helvetica* Biozone (Fig. 14).

According to Rodríguez-Tovar et al. (2009a), trace fossils from the Boquerón Member (mainly *Chondrites* and *Planolites*) suggest the recovery to pre-OAE conditions, although they identified several intervals with oxygen-depleted conditions.

6. Conclusions

Detailed analysis of foraminiferal assemblages and geochemical proxies from the Baños de la Hedionda section (South Iberian Palaeomargin) allowed us to identify the impact of OAE2 in this area of the western Tethys.

The Capas Blancas Member represents the pre-extinction phase with diverse foraminiferal assemblages and a good water-column tiering, with well-oxygenated, oligotrophic deep-waters and oxygenated to poorly oxygenated, mesotrophic surface-waters. A minor event with dysoxic conditions preceding the OAE2 is indicated by quantitative peaks of benthic (*Gavelinella*, *Glomospira* and *Praebulimina*) and planktic (*Muricohedbergella* and *Planoheterohelix*) opportunists.

The lack of foraminifera in the black radiolaritic shales (*W. archaeocretacea* Biozone) points to adverse conditions. Planktic foraminifera, mainly surface-dweller opportunists, are only recorded in the lowermost centimetres of the black shales. The enhancement in redox sensitive elements (Cr/Al, V/Al, U/Th, Mo_{EF} , Mo_{aut} , U_{EF} and U_{aut}) and increased TOC values point to depleted oxygen conditions. The increase in P/Ti values at the base of this stratigraphic interval indicates an abrupt increase in productivity. Therefore, the initial increase in the percentage of opportunist planktic foraminifera typical of poorly oxygenated environments and eutrophic conditions, and the disappearance of deep-dweller specialists (e.g. *Rotalipora*) and benthic foraminifera coincide with the onset of OAE2 as well as with high redox and palaeoproductivity proxies. High concentrations of radiolarians indicate abnormally high surface productivity probably related to changes in oceanic circulation and enhanced upwelling currents, as well as subsequent shallowing of the oxygen–minimum zone. The increase

in Mo_{EF} and Mo_{aut} indicates a decrease in oxygen availability towards euxinia in the upper part of the black radiolaritic shales. Increased bottom water ocean acidification may be required, however, to explain the post-depositional loss of planktic foraminiferal tests in the black radiolaritic shales.

The first centimetres of the Boquerón Member (*H. helvetica* Biozone) only contain benthic foraminifera, and planktic foraminifera reappear 26 cm above the base of this member. Foraminiferal assemblages are less diverse than in the Capas Blancas Member. Planktic assemblages mainly consist of intermediate-dwellers (praeglobotruncanids and dicarinellids) typical of oxygenated mesotrophic environments, opportunist surface-dwellers (whiteinellids, heterohelicids and guembelitrids) and opportunist deep-dwellers (hedbergellids) typical of poorly oxygenated waters with mesotrophic to eutrophic conditions. Benthic assemblages are dominated by opportunistic species that indicate dysoxic conditions after the OAE2.

The palaeoenvironmental perturbations related to OAE2 caused slow recovery of the foraminiferal assemblages, especially among benthic foraminifera, which display low diversity and are dominated by opportunistic species. However, the first stages of seafloor recolonization by benthic foraminifera occurred previous to the water column colonization by intermediate to deep-dwellers typical of mesotrophic to eutrophic waters. These data indicate a bottom-up recovery of environmental conditions. The subsequent proliferation of surface-dweller opportunists adapted to mesotrophic to eutrophic conditions, and the decrease in planktic foraminiferal diversity, may indicate the return to poorly oxygenated conditions in the water column towards the lower-middle part of the *H. helvetica* Biozone.

Acknowledgements

This study was conducted within the framework of the Projects CGL2014-58794-P (Spanish Ministry of Economy and Competitiveness, FEDER funds), CGL201-23077, CGL2011-22912, CGL2012-33281 and RYC-2009-04316 (Spanish Ministry of Science and Technology, FEDER funds), P11-RNM-7408 (Junta de Andalucía), and the Consolidated Group E05 (Government of Aragón and European Social Fund). Sánchez-Quiñónez thanks the Fundación Carolina (Spain) for financial support during his research stay at Zaragoza University. We thank Agustín Martín Algarra (Universidad de Granada) and Luis O'Dogherty (Universidad de Cádiz) for priceless collaboration during the sampling campaign. Critical review and suggestions of the editor Eduardo Koutsoukos and two anonymous reviewers are gratefully acknowledged.

References

- Alegret, L., 2007. Recovery of the deep-sea floor after the Cretaceous/Paleogene boundary event: the benthic foraminiferal record in the Basque-Cantabrian basin and in South-eastern Spain. *Palaeogeography, Palaeoclimatology, Palaeoecology* 255, 181–194.
- Alegret, L., Thomas, E., Lohmann, K.C., 2012. End-Cretaceous marine mass extinction not caused by productivity collapse. *Proceedings of the National Academy of Sciences* 109, 728–732.
- Ando, A., Huber, B.T., MacLeod, K.G., 2010. Depth-habitat reorganization of planktonic foraminifera across the Albian/Cenomanian boundary. *Paleobiology* 36, 357–373.
- Arthur, M.A., Jenkyns, H.C., Brumsack, H.J., Schlanger, S.O., 1990. Stratigraphy, geochemistry, and paleoceanography of organic carbon-rich Cretaceous sequences. In: Ginsburg, R.N., Beaudoin, B. (Eds.), *Cretaceous Resources, Events and Rhythms: Background and Plans for Research*, NATO ASI Series, pp. 75–119.
- Bak, K., Bak, M., Geroch, S., Manecki, M., 1997. Biostratigraphy and paleoenvironmental analysis of benthic foraminifera and radiolarians in Paleogene variegated shales in the Skole Unit, Polish Flysch Carpathians. *Annales Societatis Geologorum Poloniae* 67, 135–154.
- Berner, R.A., Raiswell, R., 1983. Burial of organic carbon and pyrite sulfur in sediments over Phanerozoic time: a new theory. *Geochimica et Cosmochimica Acta* 47, 855–862.

- Bernhard, J.M., 1986. Characteristic assemblages and morphologies of benthic foraminifera from anoxic, organic rich deposits: Jurassic trough Holocene. *Journal of Foraminiferal Research* 16, 207–215.
- Bornemann, A., Norris, R.D., Friedrich, O., Beckmann, B., Schouten, R., Sinningh-Damste, J., Vogel, J., Hofmann, P., Wagner, T., 2008. Isotopic evidence for glaciation during the Cretaceous super-greenhouse. *Science* 319, 951–954.
- Buzas, M.A., Culver, S.J., Jorissen, F.J., 1993. A statistical evaluation of the microhabitats of living (stained) infaunal benthic foraminifera. *Marine Micropaleontology* 29, 73–76.
- Calvert, S.E., 1990. Geochemistry and origin of the Holocene sapropel in the Black Sea. In: Ittekkot, V., Kempe, S., Michaelis, W., Spitz, A. (Eds.), *Facets of Modern Biogeochemistry*. Springer, Berlin, pp. 326–352.
- Calvert, S.E., Fontugne, M.R., 2001. On the late Pleistocene–Holocene sapropel record of climatic and oceanographic variability in the eastern Mediterranean. *Paleoceanography* 16, 78–94.
- Calvert, S.E., Pedersen, T.F., 1993. Geochemistry of recent oxic and anoxic marine sediments: implications for the geological record. *Marine Geology* 113, 67–88.
- Caron, M., Dall'Agnolo, S., Accarie, H., Barrera, E., Kauffman, E.G., Amédéo, F., Robaszynski, F., 2006. High-resolution stratigraphy of the Cenomanian Turonian boundary interval at Pueblo (USA) and wadi Bahloul (Tunisia): stable isotope and bio-events correlation. *Geobios* 39, 171–200.
- Cocconi, R., Luciani, V., 2004. Planktonic foraminifera and environmental changes across the Bonarelli Event (OAE2, Latest Cenomanian) in its type area: a high-resolution study from the Tethyan reference Bottaccione section (Gubbio, Central Italy). *Journal of Foraminiferal Research* 34, 109–129.
- Cocconi, R., Fabbucci, L., Galeotti, S., 1993. Terminal Cretaceous deep-water benthic foraminiferal decimation, survivorship and recovery at Caravaca (SE Spain). *Paleoceanology* 3, 3–24.
- Corliss, B.H., 1985. Microhabitats of benthic foraminifera within deep-sea sediments. *Nature* 314, 435–438.
- Corliss, B.H., Chen, C., 1988. Morphotype patterns of Norwegian Sea deep-sea benthic foraminifera and ecological implications. *Geology* 16, 716–719.
- Coxall, H.K., Wilson, P.A., Pearson, P.N., Sexton, P.F., 2007. Iterative evolution of digitate planktonic foraminifera. *Paleobiology* 33, 495–516.
- Dupraz, C., Strasser, A., 1999. Microbialites and micro-encrusters in shallow coral bioherms (Middle to Late Oxfordian, Swiss Jura Mountains). *Facies* 40, 101–130.
- Eicher, D.L., Worstell, P., 1970. Cenomanian and Turonian foraminifera from the Great Plains, United States. *Micropaleontology* 16, 269–324.
- Erba, E., 2004. Calcareous nannofossils and Mesozoic oceanic anoxic events. *Marine Micropaleontology* 52, 85–106.
- Erba, E., Bottini, C., Faucher, G., 2013. Cretaceous large igneous provinces: the effects of submarine volcanism on calcareous nannoplankton. *Mineralogical Magazine* 77, 1044.
- Flores, J.A., Sierro, F.J., Filippelli, G.M., Barcena, M.A., Pérez-Folgado, M., Vázquez, A., Utrilla, R., 2005. Surface water dynamics and phytoplankton communities during deposition of cyclic late Messinian sapropel sequences in the western Mediterranean. *Marine Micropaleontology* 56, 50–79.
- Fontanier, C., Jorissen, F.J., Licari, L., Alexandre, A., Anschutz, P., Carbonel, P., 2002. Live benthic foraminiferal faunas from the Bay of Biscay: faunal density, composition and microhabitats. *Deep-Sea Research. Part 1. Oceanographic Research Papers* 49, 751–785.
- Friedrich, O., Erbacher, J., 2006. Benthic foraminiferal assemblages from Demerara Rise (ODP Leg 207, western Tropical Atlantic): possible evidence for a progressive opening of the Equatorial Atlantic Gateway. *Cretaceous Research* 27, 377–397.
- Friedrich, O., Erbacher, J., Wilson, P.A., Moriya, K., Mutterlose, J., 2009. Paleoenvironmental changes across the Mid Cenomanian Event in the tropical Atlantic Ocean (Demerara Rise, ODP Leg 207) inferred from benthic foraminiferal assemblages. *Marine Micropaleontology* 71, 28–40.
- Gallego-Torres, D., Martínez-Ruiz, F., Paytan, A., Jiménez-Espejo, F.J., Ortega-Huertas, M., 2007. Pliocene–Holocene evolution of depositional conditions in the eastern Mediterranean: Role of anoxia vs. productivity at 632 time of sapropel deposition. *Palaeogeography, Palaeoclimatology, Palaeoecology* 246, 424–439.
- Gebhardt, H., Kuhnt, W., Holbourn, A., 2004. Foraminiferal response to sea level change, organic flux and oxygen deficiency in the Cenomanian of the Tarfaya Basin, southern Morocco. *Marine Micropaleontology* 53, 133–157.
- Gebhardt, H., Friederich, O., Schenk, B., Fox, L., Hart, M., Wägreich, M., 2010. Paleooceanographic changes at the northern Tethyan margin during the Cenomanian–Turonian Oceanic Anoxic Event (OAE2). *Marine Micropaleontology* 77, 25–45.
- Gertsch, B., Keller, G., Adatte, T., Berner, Z., Kassab, A.S., Tantawy, A.A.A., El-Sabbagh, A.M., Stueben, D., 2010. Cenomanian–Turonian transition in a shallow water sequence of the Sinai, Egypt. *International Journal of Earth Sciences* 99, 165–182.
- González-Donoso, J.M., Linares, D., Martín-Algarra, A., Rebollo, M., Serrano, F., Vera, J.A., 1983. Discontinuidades estratigráficas durante el Cretácico en el Península (Cordillera Bética). *Estudios Geológicos* 39, 71–116.
- Gooday, A., 2003. Benthic foraminifera (Protista) as tools in deep-water palaeoceanography: environmental influences on faunal characteristics. *Advances in Biology* 46, 1–90.
- Gupta, L.P., Kawahata, H., 2006. Downcore diagenetic changes in organic matter and implications for paleoproductivity estimates. *Global and Planetary Change* 53, 122–136.
- Gustafsson, M., Holbourn, A., Kuhnt, W., 2003. Changes in Northeast Atlantic temperature and carbon flux during the Cenomanian/Turonian paleoceanographic event: the Goban Spur stable isotope record. *Palaeogeography, Palaeoclimatology, Palaeoecology* 201, 51–66.
- Hallam, A., 1992. *Phanerozoic Sea Level Changes*. Columbia Press, New York, 266 pp.
- Hanagata, S., Nobuhara, T., 2015. Illustrated guide to Pliocene foraminifera from Miyakojima, Ryukyu Island Arc, with comments on biostratigraphy. *Palaeontologia Electronica* 18, 1.3A, 1–140.
- Hart, M.B., 1996. Recovery of the food chain after the late Cenomanian extinction event. In: Hart, M.B. (Ed.), *Biotic recovery from Mass Extinction Events*, Geological Society of London Sp. Publ. 102, pp. 265–277.
- Hart, M.B., 1999. The evolution and diversity of Cretaceous planktonic foraminifera. *Geobios* 32, 247–255.
- Hart, M.B., Bailey, H.W., 1979. The distribution of planktonic Foraminifera in the Mid-Cretaceous of NW Europe. In: Wiedmann, J. (Ed.), *Aspekte der Kreide Europas*. International Union of Geological Sciences, Series A 6, pp. 527–542.
- Haynes, S.J., Huber, B.T., MacLeod, K.G., 2015. Evolution and phylogeny of mid-Cretaceous (Albian–Coniacian) Biserial planktic foraminifera. *Journal of Foraminiferal Research* 45, 42–81.
- Holbourn, A., Kuhnt, W., 2002. Cenomanian–Turonian palaeoceanographic change on the Kerguelen Plateau—a comparison with Northern Hemisphere records. *Cretaceous Research* 23, 333–349.
- Holbourn, A., Kuhnt, W., Erbacher, J., 2001. Benthic foraminifera from lower Albian black shales (Site 1049, ODP leg 171): evidence for a non ‘uniformitarian’ record. *Journal of Foraminiferal Research* 31, 60–74.
- Huber, B.T., Petrizzo, M.R., 2014. Evolution and taxonomic study of the Cretaceous planktic foraminiferal genus *Helvetoglobotruncana* Reiss, 1957. *Journal of Foraminiferal Research* 44, 40–57.
- Huber, B.T., Leckie, R.M., Norris, R.D., Bralower, T.J., CoBabe, E., 1999. Foraminiferal assemblages and stable isotopic change across the Cenomanian–Turonian boundary in the subtropical North Atlantic. *Journal of Foraminiferal Research* 29, 392–417.
- Huber, B.T., Norris, R.D., McLeod, K.G., 2002. Deep-sea paleotemperature record of extreme warmth during the Cretaceous. *Geology* 30, 123–126.
- Ingall, E.D., Bustin, R.M., Van Cappellen, P., 1993. Influence of water column anoxia on the burial and preservation of carbon and phosphorus in marine shales. *Geochimica et Cosmochimica Acta* 57, 303–316.
- Jarvis, I., Carson, G.A., Cooper, M.K.E., Hart, M.B., Leary, P.N., Tocher, B.A., Horne, D., Rosenfeld, A., 1988. Microfossil assemblages and the Cenomanian–Turonian (Late Cretaceous) oceanic anoxic event. *Cretaceous Research* 9, 3–103.
- Jones, R.W., Charnock, M.A., 1985. “Morphogroups” of agglutinated foraminifera. Their life positions and feeding habits and potential applicability in (Paleo) Ecological studies. *Revue de Paléobiologie* 4, 311–320.
- Jones, B.A., Manning, D.A.C., 1994. Comparison of geochemical indices used for the interpretation of paleoredox conditions in ancient mudstones. *Chemical Geology* 111, 111–129.
- Jorissen, F.J., De Stigter, H.C., Widmark, J.G.V., 1995. A conceptual model explaining benthic foraminiferal habitats. *Marine Micropaleontology* 26, 3–15.
- Jorissen, F.J., Fontanier, C., Thomas, E., 2007. Paleooceanographic proxies based on deep-sea benthic foraminiferal assemblage characteristics. In: Hillaire-Marcel, C., de Vernal, A. (Eds.), *Proxies in Late Cenozoic Paleoclimatology (Pt2)*, Biological Tracers and Biomarkers. Elsevier, Amsterdam, pp. 263–326.
- Kaiho, K., 1994. Planktonic and benthic foraminiferal extinction events during the last 100 m.y. *Palaeogeography, Palaeoclimatology, Palaeoecology* 111, 45–71.
- Kaiho, K., 1999. Evolution in the test size of deep-sea benthic foraminifera during the past 120 m.y. *Marine Micropaleontology* 37, 53–65.
- Kędzierski, M., Machaniec, E., Rodríguez-Tovar, F.J., Uchman, A., 2012. Bio-events, foraminiferal and nannofossil biostratigraphy of the Cenomanian/Turonian boundary interval in the Subsilesian Nappe, Rybie section, Polish Carpathians. *Cretaceous Research* 35, 181–198.
- Keller, G., Pardo, A., 2004a. Disaster opportunists Guembeltrinitidae: index for environmental catastrophes. *Marine Micropaleontology* 53, 83–116.
- Keller, G., Pardo, A., 2004b. Age and environment of the Cenomanian–Turonian global stratotype section and point at Pueblo, Colorado. *Marine Micropaleontology* 51, 95–128.
- Keller, G., Han, Q., Adatte, T., Burns, S.J., 2001. Paleoenvironment of the Cenomanian–Turonian transition at Eastbourne, England. *Cretaceous Research* 22, 391–422.
- Kennedy, W.J., Walaszczyk, I., Cobban, W.A., 2005. The Global Boundary Stratotype Section and Point for the base of the Turonian Stage of the Cretaceous: Pueblo, Colorado, U.S.A. *Episodes* 28, 93–104.
- Klein, C., Mutterlose, J., 2001. Benthic foraminifera: indicators for a long-term improvement of living conditions in the late Valanginian of the NW German Basin. *Journal of Micropaleontology* 20, 81–95.
- Koutsoukos, E.A.M., Leary, P.N., Hart, M.B., 1990. Latest Cenomanian–earliest Turonian low-oxygen tolerant benthic foraminifera: a case-study from the Serpige basin (NE Brazil) and the western Anglo-Paris basin (southern England). *Palaeogeography, Palaeoclimatology, Palaeoecology* 77, 145–177.
- Kuroda, J., Ogawa, N.O., Tanimizu, M., Coffin, M.T., Tokuyama, H., Kitazato, H., Ohkouchi, N., 2007. Contemporaneous massive subaerial volcanism and late Cretaceous Oceanic Anoxic Event 2. *Earth and Planetary Science Letters* 256, 211–223.
- Kuypers, M.M.M., Pancost, R.D., Nijenhuis, I.A., Sinningh-Damste, J.S., 2002. Enhanced productivity led to increased organic carbon burial in the euxinic North Atlantic Basin during the late Cenomanian oceanic anoxic event. *Paleoceanography* 17, 1051.

- Latimer, J.C., Filippelli, G.M., 2001. Terrigenous input and paleoproductivity in the Southern Ocean. *Paleoceanography* 16, 627–643.
- MacLeod, K.G., Huber, B.T., Jiménez Berrocoso, A., Wendler, I., 2013. A stable and hot Turonian without glacial $\delta^{18}\text{O}$ excursions indicated by exquisitely preserved Tanzanian foraminifera. *Geology* 41, 1083–1086.
- Martín-Algarra, A., 1987. Evolución Geológica Alpina del Contacto entre las Zonas Internas y las Zonas Externas de la Cordillera Bética. PhD thesis. Universidad de Granada, 1171 pp.
- Martín-Algarra, A., Sánchez-Navas, A., 2000. Bacterially mediated authigenesis in Mesozoic stromatolites from condensed pelagic sediments (Betic Cordillera, Southern Spain). In: Glenn, C.R., Lucas, J., Prévôt-Lucas, L. (Eds.), *Marine Authigenesis: From Global to Microbial*, SEPM Special Publication 66, pp. 499–525.
- Martín-Algarra, A., Vera, J.A., 1994. Mesozoic pelagic phosphate stromatolites from the Penibetic (Betic Cordillera, Southern Spain). In: Bertrand-Sarfati, J., Monty, C. (Eds.), *Phanerozoic Stromatolites II*. Kluwer Academic Publishers, New York, pp. 345–391.
- Monteiro, F.M., Pancost, R.D., Ridwell, A., Donnadieu, Y., 2012. Nutrients as the dominant control on the spread of anoxia and euxinia across the Cenomanian-Turonian oceanic anoxic event (OAE2): model-data comparison. *Paleoceanography* 27, PA4209.
- Mort, H.P., Adatte, T., Föllmi, K.B., Keller, G., Steinmann, P., Matera, V., Berner, Z., Stüben, D., 2007a. Phosphorous and the roles of productivity and nutrient recycling during oceanic event 2. *Geology* 35, 483–486.
- Mort, H., Jacquant, O., Adatte, T., Steinmann, P., Föllmi, K., Matera, V., Berner, Z., Stüben, D., 2007b. The Cenomanian/Turonian anoxic event at the Bonarelli Level in Italy and Spain: enhanced productivity and/or better preservation? *Cretaceous Research* 28, 597–612.
- Murray, J.W., 1991. *Ecology and Palaeoecology of Benthic Foraminifera*. Longman, Harlow, 397 pp.
- Nagao, S., Nakashima, S., 1992. Possible Complexation of Uranium with Dissolved Humic Substances in Pore Water of Marine-Sediments. *Science of the Total Environment* 118, 439–447.
- Nagy, J., 1992. Environmental significance of foraminiferal morphogroups in Jurassic North Sea deltas. *Paleoceanography, Palaeoclimatology, Palaeoecology* 95, 111–134.
- Nederbragt, A.J., Fiorentino, A., 1999. Stratigraphy and paleoceanography of the Cenomanian-Turonian Boundary Event in Oued Mellegue, north-western Tunisia. *Cretaceous Research* 20, 47–62.
- Norris, R.D., Bice, K.L., Magno, E.A., Wilson, P.A., 2002. Jiggling the tropical thermostat in the Cretaceous hothouse. *Geology* 30, 299–302.
- O'Dogherty, L., 1994. Biochronology and Paleontology of Mid-Cretaceous Radiolarians from Northern Apennines (Italy) and Betic Cordillera (Spain). In: *Mémoires de Géologie, Lausanne*, 21, pp. 1–415.
- O'Dogherty, L., Martín-Algarra, A., Gursky, H.J., Aguado, R., 2001. El horizonte radiolítico-bituminoso del límite Cenomaniense-Turonense en la Zona Subbética. *Geotemas* 3, 249–252.
- Petrizzo, M.R., 2002. Palaeoceanographic and palaeoclimatic inferences from Late Cretaceous planktonic foraminiferal assemblages from the Exmouth Plateau (ODP Sites 762 and 763, eastern Indian Ocean). *Marine Micropaleontology* 45, 117–150.
- Peryt, D., 2004. Benthic foraminiferal response to the Cenomanian-Turonian and Cretaceous-Paleogene boundary events. *Przegląd Geologiczny* 52, 827–832.
- Peryt, D., Lamolda, M., 1996. Benthonic foraminiferal mass extinction and survival assemblages from the Cenomanian-Turonian Boundary Event in the Menoyo section, northern Spain. *Geological Society, London, Special Publications* 102, pp. 245–258.
- Plewa, K., Meggers, H., Kasten, S., 2006. Barium in sediments off northwest Africa: a tracer for palaeoproductivity or meltwater events? *Paleoceanography* 21, PA2015.
- Pogge von Strandmann, P.A.E., Jenkyns, H.C., Woodfine, R.G., 2013. Lithium isotope evidence for enhanced weathering during Oceanic Anoxic Event 2. *Nature Geoscience* 6, 668–672.
- Powell, W.G., Johnston, P.A., Collom, C.J., 2003. Geochemical evidence for oxygenated bottom waters during deposition of fossiliferous strata of the Burgess Shale Formation. *Paleoceanography, Palaeoclimatology, Palaeoecology* 201, 249–268.
- Price, G.D., Hart, M.B., 2002. Isotopic evidence for early to mid-Cretaceous ocean temperature variability. *Marine Micropaleontology* 46, 45–58.
- Reolid, M., Martínez-Ruiz, F., 2012. Comparison of benthic foraminifera and geochemical proxies in shelf deposits from the Upper Jurassic of the Prebetic (southern Spain). *Journal of Iberian Geology* 38, 449–465.
- Reolid, M., Rodríguez-Tovar, F.J., Nagy, J., Olóriz, F., 2008a. Benthic foraminiferal morphogroups of mid to outer shelf environments of the Late Jurassic (Prebetic Zone, Southern Spain): characterisation of biofacies and environmental significance. *Paleoceanography, Palaeoclimatology, Palaeoecology* 261, 280–299.
- Reolid, M., Nagy, J., Rodríguez-Tovar, F.J., Olóriz, F., 2008b. Foraminiferal assemblages as palaeoenvironmental bioindicators in Late Jurassic epicontinental platforms: relation with trophic conditions. *Acta Palaeontologica Polonica* 53, 705–722.
- Reolid, M., Rodríguez-Tovar, F.J., Marok, A., Sebane, A., 2012a. The Toarcian Oceanic Anoxic Event in the Western Saharan Atlas, Algeria (North African Paleomargin): role of anoxia and productivity. *Geological Society of America Bulletin* 124, 1646–1664.
- Reolid, M., Rodríguez-Tovar, F.J., Nagy, J., 2012b. Ecological replacement of Valanginian agglutinated foraminifera during a maximum flooding event in the Boreal realm (Spitsbergen). *Cretaceous Research* 33, 196–204.
- Reolid, M., Sánchez-Quinónez, C.A., Alegret, L., Molina, E., 2015. Palaeoenvironmental turnover across the Cenomanian-Turonian transition in Oued Bahloul, Tunisia: Foraminifera and geochemical proxies. *Paleoceanography, Palaeoclimatology, Palaeoecology* 417, 491–510.
- Robaszynski, F., Caron, M., 1995. Foraminifères planctoniques du Crétacé: Commentaire de la zonation Europe-Méditerranée. *Bulletin de la Société géologique de France* 166 (6), 681–692.
- Robertson, A.K., Filippelli, G.M., 2008. Paleoproductivity variations in the eastern equatorial Pacific over glacial timescales: American Geophysical Union Fall Meeting 2008. Abstract PP33C-1576.
- Rodríguez-Tovar, F.J., Uchman, A., Martín-Algarra, A., 2009a. Oceanic anoxic event at the Cenomanian-Turonian boundary interval (OAE-2): ichnological approach from the Betic Cordillera, southern Spain. *Lethaia* 42, 407–417.
- Rodríguez-Tovar, F.J., Uchman, A., Martín-Algarra, A., O'Dogherty, L., 2009b. Nutrient spatial variation during intrabasinal upwelling at the Cenomanian-Turonian oceanic anoxic event in the westernmost Tethys: an ichnological and facies approach. *Sedimentary Geology* 215, 83–93.
- Sánchez-Quinónez, C.A., Alegret, L., Aguado, R., Delgado, A., Larrasoana, J.C., Martín-Algarra, A., O'Dogherty, L., Molina, E., 2010. Foraminíferos del tránsito Cenomaniense-Turonense en la sección de El Chorro, Cordillera Bética, sur de España. *Geogaceta* 49, 23–26.
- Schlanger, S.O., Jenkyns, H.C., 1976. Cretaceous oceanic anoxic events, causes and consequences. *Geologie en Mijnbouw* 55, 179–184.
- Scopelliti, G., Bellanca, A., Coccioni, R., Luciani, V., Neri, R., Baudin, F., Chiari, M., Marcucci, M., 2004. High-resolution geochemical and biotic records of the Tethyan 'Bonarelli Level' (OAE2, latest Cenomanian) from the Calabianca-Guidaloca composite section, northwestern Sicily, Italy. *Paleoceanography, Palaeoclimatology, Palaeoecology* 208, 293–317.
- Sen, A.K., Filippelli, G.M., Flores, J.A., 2008. An application of wavelet analysis to palaeoproductivity records from the Southern Ocean. *Computers and Geosciences* 35, 1445–1450.
- Sliter, W.V., 1975. Foraminiferal life and residue assemblages from Cretaceous slope deposits. *Geological Society of America Bulletin* 86, 897–906.
- Su, W., Wang, Y., Cramer, B.D., Munneke, A., Li, Z., Fu, L., 2008. Preliminary estimation of palaeoproductivity via TOC and habitat types: which method is more reliable? A case study on the Ordovician/Silurian transitional black shales of the Upper Yangtze Platform, South China. *Journal of China University of Geosciences* 19, 534–548.
- Sun, Y.B., Wu, F., Clemens, S.C., Oppo, D.W., 2008. Processes controlling the geochemical composition of the South China Sea sediments during the last climatic cycle. *Chemical Geology* 257, 234–249.
- Tribovillard, N., Algeo, T., Lyons, T., Riboulleau, A., 2006. Trace metals as palaeoredox and palaeoproductivity proxies: an update. *Chemical Geology* 232, 12–32.
- Tribovillard, N., Algeo, T.J., Baudin, F., Riboulleau, A., 2012. Analysis of marine environmental conditions based on molybdenum-uranium covariation – Applications to Mesozoic paleoceanography. *Chemical Geology* 324–325, 46–58.
- Tsandeov, I., Slomp, C.P., 2009. Modeling phosphorous cycling and carbon burial during Cretaceous Oceanic Anoxic Events. *Earth and Planetary Science Letters* 286, 71–79.
- Turgeon, S.C., Brumsack, H.J., 2006. Anoxic vs dyoxic events reflected in sediment geochemistry during the Cenomanian-Turonian Boundary Event (Cretaceous) in the Umbria-Marche basin of central Italy. *Chemical Geology* 234, 321–339.
- Turgeon, S.C., Creaser, R.A., 2008. Cretaceous oceanic anoxic event 2 triggered by a massive magmatic episode. *Nature* 454, 323–326.
- Uchman, A., Rodríguez-Tovar, F.J., Machanic, E., Kędzierski, M., 2013. Ichnological characteristics of Late Cretaceous hemipelagic and pelagic sediments on a submarine high around the OAE-2 event: a case from the Rybie section, Polish Carpathians. *Paleoceanography, Palaeoclimatology, Palaeoecology* 370, 222–231.
- Van Cappellen, P., Ingall, E.D., 1994. Benthic phosphorus regeneration, net primary production, and ocean anoxia—a model of the coupled marine biogeochemical cycles of carbon and phosphorus. *Paleoceanography* 9, 677–692.
- Van der Zwaan, G.J., Duijnste, I.A.P., Den Dulk, M., Ernst, S.R., Jannink, N.T., Kouwenhoven, T.J., 1999. Benthic foraminifera: proxies or problem? A review of palaeoclimatological concepts. *Earth-Science Reviews* 46, 213–236.
- Vera, J.A. (coord.), 2004. Zonas Externas Béticas. In: Vera, J.A. (Ed.), *Geología de España*. SGE-IGME, Madrid, 354–389.
- Wang, C.S., Hu, X.M., Jansa, L., Wan, X.Q., Tao, R., 2001. The Cenomanian-Turonian anoxic event in southern Tibet. *Cretaceous Research* 22, 481–490.
- Wendler, I., Huber, B.T., MacLeod, K.G., Wendler, J.E., 2013. Stable oxygen and carbon isotope systematics of exquisitely preserved Turonian foraminifera from Tanzania – understanding isotopic signatures in fossils. *Marine Micropaleontology* 102, 1–33.
- Widmark, J.G.V., 2000. Biogeography of terminal Cretaceous benthic foraminifera: deep-water circulation and trophic gradients in the deep South Atlantic. *Cretaceous Research* 21 (2–3), 367–379.
- Wignall, P.B., Myers, K.J., 1988. Interpreting the benthic oxygen levels in mudrocks: a new approach. *Geology* 16, 452–455.
- Zhou, L., Wignall, P.B., Su, J., Feng, Q., Xie, S., Zhao, L., Huang, J., 2012. U/Mo ratios and $\delta^{98/95}\text{Mo}$ as local and global redox proxies during mass extinction events. *Chemical Geology* 324–325, 99–197.

Appendix 1. Planktic foraminiferal species

Dicarinella algeriana (Caron, 1966)
Dicarinella canaliculata (Reuss, 1854)
Dicarinella hagni (Scheibnerova, 1962)
Dicarinella imbricata (Mornod, 1950)
Globigerinelloides bentonensis (Morrow, 1934)
Globigerinelloides ultramicrus (Subbotina, 1949)
Guembelitria cenomana (Keller, 1935)
Helvetoglobotruncana helvetica (Bolli, 1945)
Helvetoglobotruncana praehelvetica (Trujillo, 1960)
Planoheterohelix globulosa (Cushman, 1938)
Planoheterohelix moremani (Cushman, 1938)
Planoheterohelix paraglobulosa Georgescu and Huber, 2009
Marginotruncana marginata (Reuss, 1845)
Marginotruncana sigali (Reichel, 1950)
Muricohedbergella delrioensis (Carsey, 1926)
Muricohedbergella planispira (Tappan, 1940)
Muricohedbergella simplex (Morrow, 1934)
Parathalmanninella appenninica (Renz, 1936)
Praeglobotruncana delrioensis (Plummer, 1931)
Praeglobotruncana gibba Klaus, 1960
Praeglobotruncana stephani (Gandolfi, 1942)
Rotalipora cushmani (Morrow, 1934)
Rotalipora montsalvensis (Mornod, 1950)
Schackoina cenomana (Shacko, 1897)
Sigalitruncana marianosi (Douglas, 1969)
Thalmanninella brotzeni Sigal, 1948
Thalmanninella deeckeii (Franke, 1925)
Thalmanninella greenhornensis (Morrow, 1934)
Whiteinella aprica (Loeblich and Tappan, 1961)
Whiteinella archaeocretacea Pesagno, 1967
Whiteinella aumalensis (Sigal, 1952)
Whiteinella baltica Douglas and Rankin, 1969
Whiteinella brittonensis (Loeblich and Tappan, 1961)
Whiteinella inornata (Bolli, 1957)

Appendix 2. Benthic foraminiferal species

Ammodiscus spp.
Aragonia sp.
Ammosphaeroidina spp.
Arenobulimina spp.
Astacolus crepidularis (Roemer, 1842)
Astacolus gratus (Reuss, 1863)
Astacolus spp.
Bathysiphon spp.
Charltonina australis Scheibnerová, 1978
Charltonina sp.
Clavulinoides sp.
Conorotalites sp.
Coryphostoma spp.
Dorothia pupa (Reuss, 1860)

Dorothia spp.
Ellipsoidella sp.
Ellipsopolymorphina sp.
Epistomina sp.
Epistomina spinulifera (Reuss, 1862)
Frondicularia sp.
Gaudryina pyramidata Cushman, 1926
Gaudryina spp.
Gavelinella cenomanica (Brotzen, 1945)
Gavelinella spp.
Glandulina sp.
Globorotalites sp.
Globulina sp.
Glomospira spp.
Glomospirella sp.
Gubkinella graysonensis (Tappan, 1940)
Gyroidinoides beisseli (White, 1928)
Gyroidinoides globosus (Hagenow, 1842)
Gyroidinoides sp.
Gyroidinoides subglobosus Dailey, 1970
Hemirobulina sp.
Hyperammina sp.
Laevidentalina spp.
Lagena sp.
Lenticulina rotulata (Lamarck, 1804)
Lenticulina spp.
Lenticulina truncata (Reuss, 1851)
Lingulina sp.
Marginulina sp.
Marginulinopsis sp.
Marssonella oxycona (Reuss, 1860)
Oolina spp.
Patellina sp.
Plectina pinswangensis Hagn, 1953
Pleurostomella spp.
Praebulimina spp.
Pyrulina spp.
Pyrulinoidea spp.
Quadriformina sp.
Ramulina spp.
Rhabdammina sp.
Saracenaria sp.
Spiroplectammina roemeri Lalicker, 1935
Spiroplectammina sp.
Spiroplectammina spectabilis (Grzybowski, 1898)
Stensioeina exsculpta (Reuss, 1860)
Stensioeina granulata (Olbertz, 1942)
Stensioeina sp.
Tappanina selmensis (Cushman, 1933)
Tappanina sp.
Textularia sp.
Tristix sp.
Tritaxia gaultina (Morozova, 1948)
Vaginulinopsis sp.
Valvulineria sp.